



Stability analysis for pitchfork bifurcations of solitary waves in generalized nonlinear Schrödinger equations

Jianke Yang*

Department of Mathematics and Statistics, University of Vermont, Burlington, VT 05401, USA

ARTICLE INFO

Article history:

Received 12 April 2012
 Received in revised form
 12 October 2012
 Accepted 29 October 2012
 Available online 1 November 2012
 Communicated by K. Promislow

Keywords:

Solitary waves
 Pitchfork bifurcation
 Stability
 Generalized NLS equations

ABSTRACT

Linear stability of both sign-definite (positive) and sign-indefinite solitary waves near pitchfork bifurcations is analyzed for the generalized nonlinear Schrödinger equations with arbitrary forms of nonlinearity and external potentials in arbitrary spatial dimensions. Bifurcations of linear-stability eigenvalues associated with pitchfork bifurcations are analytically calculated. Based on these eigenvalue-bifurcation formulae, linear stability of solitary waves near pitchfork bifurcations is then determined. It is shown that the base solution branch switches stability at the bifurcation point. In addition, the two bifurcated solution branches and the base branch have the opposite (same) stability when their power slopes have the same (opposite) sign. Furthermore, the stability of these solution branches can be determined almost exclusively from their power diagram (especially for positive solitary waves). These stability results are also compared with the Hamiltonian–Krein index theory, and they are shown to be consistent with each other. Lastly, various numerical examples are presented, and the numerical results confirm the analytical predictions both qualitatively and quantitatively.

© 2012 Elsevier B.V. All rights reserved.

1. Introduction

Bifurcation of solitary waves is an important phenomenon in nonlinear wave equations. One type of bifurcation is the so-called pitchfork bifurcation, where a base branch of solitary waves exists on both sides of the bifurcation point, but two additional solution branches bifurcate out to only one side of the bifurcation point. The most common pitchfork bifurcation of solitary waves is the symmetry-breaking bifurcation, where solitary waves on the base branch have certain symmetry, but solitary waves on the bifurcated branches lose that symmetry and become asymmetric. This symmetry-breaking bifurcation occurs frequently in various nonlinear wave models originating from diverse physical disciplines (such as nonlinear optics and Bose–Einstein condensates). For instance, this bifurcation has been reported in the nonlinear Schrödinger (NLS) equations with external potentials [1–11]. Physically these NLS equations govern nonlinear light propagation in refractive-index-modulated optical media [12,13] and atomic interaction in Bose–Einstein condensates loaded in magnetic or optical traps (in the latter community these equations are called the Gross–Pitaevskii equations [14]). This symmetry-breaking bifurcation has also been reported in the linearly-coupled NLS equations which govern light transmission

in dual-core couplers [15,16]. Analytical studies of symmetry-breaking bifurcations have also been made, mostly for the NLS equations with special types of nonlinearities and potentials (see [1,4,6,8,9,11] for instance). In [1] the authors considered a one-dimensional NLS equation with focusing cubic nonlinearity and a Dirac-type symmetric double-well potential, and showed the presence of symmetry breaking bifurcation as well as the exchange of dynamical stability from the symmetric branch to the asymmetric branch at the bifurcation point. In [4] the authors considered a class of multi-dimensional NLS equations with focusing cubic nonlinearity and symmetric potentials, and showed that symmetry-breaking bifurcation occurs when the power (also called the squared norm in mathematics and particle numbers in Bose–Einstein condensation) of the symmetric solitary waves increases above a certain threshold, provided that the first two eigenvalues of the linear potential are sufficiently close to each other (such as in double-well potentials with large separation between the two wells). In addition, the authors showed that above this power threshold, the symmetric states become unstable, and a pair of orbitally stable asymmetric states appear. In [6], the author considered a class of multi-dimensional NLS equations with defocusing power nonlinearity and symmetric double-well potentials in the semiclassical limit, and showed that symmetry-breaking bifurcations occur for antisymmetric solitary waves. In [8], the authors considered a class of one-dimensional NLS equations with focusing power nonlinearity and a symmetric potential, and showed that symmetry-breaking bifurcation occurs for positive symmetric solitary waves if the

* Tel.: +1 8026564314; fax: +1 8026562552.
 E-mail address: jyang@math.uvm.edu.

potential satisfies certain requirements. In addition, they showed that the symmetric branch changes stability at the bifurcation point, and the asymmetric branches can be orbitally stable or unstable under different conditions. In [9], the authors considered the same class of equations as in [8] and obtained normal forms for these symmetry-breaking bifurcations. In [11], this author considered the general class of NLS equations with arbitrary forms of nonlinearities and potentials in arbitrary spatial dimensions, and derived the general analytical conditions for pitchfork bifurcations as well as the power formulae for solitary-wave branches near the pitchfork bifurcation point.

In this paper, we consider the general nonlinear Schrödinger equations with arbitrary forms of nonlinearity and potentials in arbitrary spatial dimensions (as in [11]). These equations include the Gross–Pitaevskii equations in Bose–Einstein condensates with attractive or repulsive atomic interactions and nonlinear light-transmission equations in linear potentials or nonlinear lattices with power or non-power nonlinearities as special cases [12–14,17]. For this large class of equations, we determine the linear stability of both sign-definite (positive) and sign-indefinite solitary waves near pitchfork bifurcations. Our strategy is to explicitly calculate the bifurcation of linear-stability eigenvalues from the origin, which always takes place whenever a pitchfork bifurcation occurs (see Theorem 3 in Section 3). It turns out that this eigenvalue bifurcation from the origin is intimately related to the power slopes of solution branches at the bifurcation point. This finding enables us to determine the linear stability of solution branches from the shape of the power diagram.

Based on this eigenvalue bifurcation from the origin and assuming no other instabilities interfere, linear stability of solitary waves near pitchfork bifurcations is then obtained (see Theorem 4 in Section 3). We show that the base solution branch always switches stability at the bifurcation point. In addition, the bifurcated solution branches and the base branch have opposite (same) stability when their power slopes have the same (opposite) sign. Furthermore, the stability of these solution branches can be determined almost exclusively from their power diagram (especially for positive solitary waves, see Theorem 5). These stability results are also compared with the Hamiltonian–Krein index theory, and they are shown to be consistent with each other. Lastly, we present various numerical examples which contain double-well or periodic potentials and focusing or defocusing nonlinearities of Kerr (cubic) or non-Kerr types. These numerical results confirm the analytical predictions both qualitatively and quantitatively.

One unusual feature on the linear stability of these pitchfork bifurcations is that the base and bifurcated solution branches (on the same side of the bifurcation point) can be both stable or both unstable, which contrasts such bifurcations in finite-dimensional dynamical systems where the base and bifurcated branches generally have opposite stability [18].

Compared with the earlier analytical results on stability of pitchfork bifurcations (such as in [1,4,6,8]), our stability results have the following three distinctive features. First, our results apply to the general NLS equations with no restriction on the nonlinearity, potential or spatial dimensions. Second, we established a direct link between linear stability and the shape of the power diagram. Third, we derived explicit analytical formulae for linear-stability eigenvalues of solitary waves, which can be useful when quantitative prediction of linear instability is needed.

2. Preliminaries

We consider the generalized nonlinear Schrödinger (GNLS) equations with arbitrary forms of nonlinearity and external

potentials in arbitrary spatial dimensions. These equations can be written as

$$iU_t + \nabla^2 U + F(|U|^2, \mathbf{x})U = 0, \tag{2.1}$$

where $\nabla^2 = \partial^2/\partial x_1^2 + \partial^2/\partial x_2^2 + \dots + \partial^2/\partial x_N^2$ is the Laplacian in the N -dimensional space $\mathbf{x} = (x_1, x_2, \dots, x_N)$, and $F(\cdot, \cdot)$ is a general real-valued function which includes nonlinearity as well as external potentials. These GNLS equations include the Gross–Pitaevskii equations in Bose–Einstein condensates [14] and nonlinear light-transmission equations in linear potentials and nonlinear lattices [12,13,17,19] as special cases. Notice that these equations are conservative and Hamiltonian.

For a large class of nonlinearities and potentials, this equation admits stationary solitary waves

$$U(\mathbf{x}, t) = e^{i\mu t} u(\mathbf{x}), \tag{2.2}$$

where $u(\mathbf{x})$ is a real and localized function in the square-integrable functional space which satisfies the equation

$$\nabla^2 u - \mu u + F(u^2, \mathbf{x})u = 0, \tag{2.3}$$

and μ is a real-valued propagation constant. Examples of such solitary waves can be found in numerous books and articles (see [12,13] for instance). In these solitary waves, μ is a free parameter, and $u(\mathbf{x})$ depends continuously on μ . Under certain conditions, these solitary waves undergo bifurcations at special values of μ . Three major types of bifurcations have been classified [11]. Of these bifurcations, stability of solitary waves near saddle–node bifurcations has been analyzed in [20,21]. It was shown that no stability switching takes place at a saddle–node bifurcation, which dispels a pervasive misconception that such stability switching should occur. In this paper, we study the stability of solitary waves near pitchfork bifurcations.

A pitchfork bifurcation in Eq. (2.1) is where on one side of the bifurcation point $\mu = \mu_0$, there is a single solitary wave branch $u^0(\mathbf{x}; \mu)$; but on the other side of μ_0 , three distinct solitary-wave branches appear. One of them is a smooth continuation of the $u^0(\mathbf{x}; \mu)$ branch, but the other two branches $u^\pm(\mathbf{x}; \mu)$ are new and they bifurcate out at $\mu = \mu_0$. In this paper, the $u^0(\mathbf{x}; \mu)$ branch will be called the base branch, and the $u^\pm(\mathbf{x}; \mu)$ branches will be called the bifurcated branches.

To present conditions for pitchfork bifurcations, we introduce the linearization operator of Eq. (2.3),

$$L_1 = \nabla^2 - \mu + \partial_u[F(u^2, \mathbf{x})u], \tag{2.4}$$

which is a linear Schrödinger operator. We also introduce the standard inner product of functions,

$$\langle f, g \rangle = \int_{-\infty}^{\infty} f^*(\mathbf{x})g(\mathbf{x})d\mathbf{x},$$

where the superscript ‘*’ represents complex conjugation. In addition, we define the power of a solitary wave $u(\mathbf{x}; \mu)$ as

$$P(\mu) = \langle u, u \rangle = \int_{-\infty}^{\infty} u^2(\mathbf{x}; \mu)d\mathbf{x},$$

and denote the power functions of the base and bifurcated solution branches as

$$P_0(\mu) \equiv \langle u^0(\mathbf{x}; \mu), u^0(\mathbf{x}; \mu) \rangle, \\ P_\pm(\mu) \equiv \langle u^\pm(\mathbf{x}; \mu), u^\pm(\mathbf{x}; \mu) \rangle.$$

If a bifurcation occurs at $\mu = \mu_0$, by denoting the corresponding solitary wave and the L_1 operator as

$$u_0(\mathbf{x}) \equiv u(\mathbf{x}; \mu_0), \quad L_{10} \equiv L_1|_{\mu=\mu_0, u=u_0},$$

then L_{10} should have a discrete zero eigenvalue. This is a necessary condition for all bifurcations, not just for pitchfork bifurcations. In [11], the following sufficient conditions for pitchfork bifurcations were derived.

Theorem 1. Assume that zero is a simple discrete eigenvalue of L_{10} . Denote the real eigenfunction of this zero eigenvalue as $\psi(\mathbf{x})$, and denote

$$G(u; \mathbf{x}) \equiv F(u^2; \mathbf{x})u, \quad G_k(\mathbf{x}) \equiv \partial_u^k G|_{u=u_0}, \quad k = 2, 3. \quad (2.5)$$

Then if

$$\langle u_0, \psi \rangle = \langle G_2, \psi^3 \rangle = 0, \quad (2.6)$$

$$R \equiv \langle 1 - G_2 L_{10}^{-1} u_0, \psi^2 \rangle \neq 0, \quad (2.7)$$

and

$$S \equiv \langle G_3, \psi^4 \rangle - 3\langle G_2 \psi^2, L_{10}^{-1} (G_2 \psi^2) \rangle \neq 0, \quad (2.8)$$

a pitchfork bifurcation occurs at $\mu = \mu_0$. The new solitary waves $u^\pm(\mathbf{x}; \mu)$ bifurcate to the right (left) side of $\mu = \mu_0$ if the constants R and S have the same (opposite) sign.

Note. The above theorem was derived under the assumption that the function $F(u^2; \mathbf{x})$ is infinitely differentiable with respect to u (this assumption was implicitly made but not explicitly stated in [11]). Under this assumption, the base solution branch $u^0(\mathbf{x}; \mu)$ is infinitely differentiable with respect to μ , and the bifurcated solution branches $u^\pm(\mathbf{x}; \mu)$ are infinitely differentiable with respect to $\sqrt{\mu - \mu_0}$, due to the power series of these solutions obtained in [11].

In [11], slopes of power functions for the base and bifurcated solitary-wave branches at the pitchfork bifurcation point were also derived.

Theorem 2. Suppose the conditions in Theorem 1 hold and a pitchfork bifurcation occurs at $\mu = \mu_0$. Then power slopes of the base and bifurcated solitary-wave branches at the bifurcation point are given as

$$P'_0(\mu_0) = 2\langle u_0, L_{10}^{-1} u_0 \rangle, \quad (2.9)$$

and

$$P'_+(\mu_0) = P'_-(\mu_0) = P'_0(\mu_0) + \frac{6R^2}{S}. \quad (2.10)$$

Here (and in later text) the prime represents the derivative.

In this article, we consider pitchfork bifurcations in the GNLS equations (2.1) where the bifurcation conditions in Theorem 1 hold.

The main goal of this paper is to determine the linear stability of solitary waves near these pitchfork bifurcations. To study this linear stability, we perturb the solitary waves as [13, p. 176]

$$U(\mathbf{x}, t) = e^{i\mu t} \left\{ u(\mathbf{x}) + [v(\mathbf{x}) + w(\mathbf{x})]e^{\lambda t} + [v^*(\mathbf{x}) - w^*(\mathbf{x})]e^{\lambda^* t} \right\}, \quad (2.11)$$

where $v, w \ll 1$ are normal-mode perturbations, and λ is the mode's eigenvalue. Inserting this perturbed solution into (2.1) and linearizing, we obtain the following linear eigenvalue problem

$$\mathcal{L}\Phi = -i\lambda\Phi, \quad (2.12)$$

where

$$\mathcal{L} = \begin{bmatrix} 0 & L_0 \\ L_1 & 0 \end{bmatrix}, \quad \Phi = \begin{bmatrix} v \\ w \end{bmatrix}, \quad (2.13)$$

$$L_0 = \nabla^2 - \mu + F(u^2, \mathbf{x}), \quad (2.14)$$

and L_1 is as defined in Eq. (2.4). Both L_0 and L_1 are linear Schrödinger operators and are Hermitian. In the later text, operator \mathcal{L} will be called the linear-stability operator. The eigenvalue problem (2.12) can also be written as

$$L_0 w = -i\lambda v, \quad L_1 v = -i\lambda w. \quad (2.15)$$

If this linear-stability eigenvalue problem admits eigenvalues λ whose real parts are positive, then the corresponding normal-mode perturbation in Eq. (2.11) exponentially grows, hence the solitary wave $u(\mathbf{x})$ is linearly unstable. Otherwise it is linearly stable. Notice that eigenvalues of this linear-stability problem always appear in quadruples $(\lambda, -\lambda, \lambda^*, -\lambda^*)$ when λ is complex, or in pairs $(\lambda, -\lambda)$ when λ is real or purely imaginary.

Using the L_0 operator, the solitary wave equation (2.3) can be written as

$$L_0 u = 0. \quad (2.16)$$

Differentiating this equation with respect to μ , we find that

$$L_1 u_\mu = u, \quad (2.17)$$

where $u_\mu \equiv \partial u / \partial \mu$. These two relations will be useful in later analysis. Due to (2.16), the linear-stability eigenvalue problem (2.15) admits a zero eigenmode for every solitary wave $u(\mathbf{x}; \mu)$:

$$\lambda = 0, \quad v = 0, \quad w = u. \quad (2.18)$$

This zero eigenmode is related to the phase invariance of the GNLS equations (2.1), which says that if $U(\mathbf{x}, t)$ is a solution of (2.1), so is $U(\mathbf{x}, t)e^{i\theta}$ for any real phase constant θ .

The GNLS equations (2.1) may be viewed as an infinite-dimensional dynamical system, with solitary waves (2.2) being its fixed points. In this view, it is tempting to deduce the stability of pitchfork bifurcations in the GNLS equations (2.1) from those in finite-dimensional dynamical systems. In finite-dimensional dynamical systems, it has been shown that at a pitchfork bifurcation point, the base fixed-point branch changes its stability. In addition, the two bifurcated fixed-point branches have the opposite stability of the base fixed-point branch (on the same side of the bifurcation point) [18]. However, these stability results were derived under the assumption that zero is a simple eigenvalue of the Jacobian (linearization) matrix of the system at the bifurcation point (see Ref. [18, Theorem 3.4.1, Hypothesis SN1]). For the GNLS equations (2.1), the counterpart of the Jacobian matrix is the linear-stability operator \mathcal{L} defined in Eq. (2.13), but zero is *not* a simple eigenvalue of \mathcal{L} at the bifurcation point (see Eq. (3.5) below). This means that we cannot apply the above stability results from finite-dimensional dynamical systems to pitchfork bifurcations in the GNLS equations (2.1). Instead we have to analyze this stability for Eq. (2.1) separately. As we will see, stability for pitchfork bifurcations in Eq. (2.1) shows novel features which do not exist in finite-dimensional dynamical systems. It is relevant to mention that the same phenomenon occurs for saddle-node bifurcations as well, where it was shown in [20,21] that no stability switching occurs in the GNLS equations (2.1) even though such stability switching generally takes place in finite-dimensional dynamical systems [18].

3. Main results

Our stability analysis starts with the basic fact that, at a pitchfork bifurcation point $\mu = \mu_0$, L_{10} has a discrete zero eigenvalue (see earlier text). With the eigenfunction of this zero eigenvalue denoted as $\psi(\mathbf{x})$ (see Theorem 1), we have

$$L_{10}\psi = 0. \quad (3.1)$$

Thus at the bifurcation point $\mu = \mu_0$, in addition to the phase-invariance-induced zero eigenmode (2.18), the linear-stability eigenvalue problem (2.15) also admits a bifurcation-induced zero eigenmode,

$$\lambda = 0, \quad v = \psi, \quad w = 0. \quad (3.2)$$

Away from the bifurcation point ($\mu \neq \mu_0$), while the phase-related zero eigenvalue (2.18) remains at the origin, the bifurcation-induced zero eigenvalue (3.2) bifurcates out since zero is not an

eigenvalue in L_1 any more (see Lemma 1 in Section 4). Thus our approach is to analytically calculate how this bifurcation-induced zero eigenvalue moves out of the origin when μ moves away from μ_0 . We will show that this zero eigenvalue only bifurcates out along the real or imaginary axis as a $\pm\lambda$ pair. Bifurcation along the real axis creates instability, while bifurcation along the imaginary axis does not create instability. Thus, based on which direction this zero eigenvalue bifurcates and assuming no other instabilities interfere, linear-stability behaviors of solitary waves near the bifurcation point will be analytically obtained. An important feature of this zero-eigenvalue bifurcation is that the bifurcated eigenvalues are intimately related to the power slopes of solution branches at the bifurcation point. This opens the door for us to determine linear stability from the shape of the power diagram. In the special case of positive solitary waves, we will show that there are indeed no other instabilities interfering near a pitchfork bifurcation, and linear stability of these waves can be read off directly from the power diagram.

For later analysis, we introduce two additional notations,

$$L_{00} \equiv L_0|_{\mu=\mu_0, u=u_0}, \quad \mathcal{L}_0 \equiv \mathcal{L}|_{\mu=\mu_0, u=u_0}. \quad (3.3)$$

In view of Eq. (2.16), we have

$$L_{00}u_0 = 0, \quad (3.4)$$

thus zero is a discrete eigenvalue of L_{00} . From Eqs. (2.18) and (3.2), we have

$$\mathcal{L}_0 \begin{bmatrix} 0 \\ u_0 \end{bmatrix} = \mathcal{L}_0 \begin{bmatrix} \psi \\ 0 \end{bmatrix} = 0, \quad (3.5)$$

so zero is also a (multifold) discrete eigenvalue of \mathcal{L}_0 .

On the bifurcation of the zero eigenvalue in the linear-stability operator \mathcal{L} when $\mu \neq \mu_0$, we have the following main results.

Theorem 3. Assume that zero is a simple discrete eigenvalue of L_{00} and L_{10} . Near a pitchfork bifurcation point $\mu = \mu_0$ in Theorem 1, if

$$\langle \psi, L_{00}^{-1} \psi \rangle \neq 0, \quad P'_0(\mu_0) \neq 0, \quad P'_\pm(\mu_0) \neq 0, \quad (3.6)$$

then a single pair of non-zero eigenvalues $\pm\lambda$ in \mathcal{L} bifurcate out along the real or imaginary axis from the origin when $\mu \neq \mu_0$;

(a) on the base solution branch $u^0(\mathbf{x}; \mu)$, the bifurcated eigenvalues λ^0 are given asymptotically by

$$(\lambda^0)^2 \rightarrow \alpha(\mu - \mu_0), \quad \mu \rightarrow \mu_0, \quad (3.7)$$

where the real constant α is

$$\alpha = \frac{R}{\langle \psi, L_{00}^{-1} \psi \rangle} \neq 0; \quad (3.8)$$

(b) on the two bifurcated solution branches $u^\pm(\mathbf{x}; \mu)$, the bifurcated eigenvalues λ^\pm are given asymptotically by

$$(\lambda^\pm)^2 \rightarrow \beta(\mu - \mu_0), \quad \mu \rightarrow \mu_0, \quad (3.9)$$

where the real constant β is

$$\beta = -2\alpha \frac{P'_\pm(\mu_0)}{P'_0(\mu_0)} \neq 0. \quad (3.10)$$

Remark 1. The present problem does not involve multi-scale wave coupling. This allows us to calculate eigenvalue bifurcations from the origin in \mathcal{L} when $0 < |\mu - \mu_0| \ll 1$ by perturbation series expansions (without worrying about effects beyond all orders of the perturbation expansion [13,22–26]).

Remark 2. In this theorem, the assumption of zero being a simple discrete eigenvalue of L_{00} and L_{10} is satisfied in all one-dimensional bifurcations and many higher-dimensional bifurcations.

A direct consequence of Theorem 3 is the following Theorem 4 which summarizes the qualitative linear-stability properties of solitary waves near a pitchfork bifurcation point.

Theorem 4. Suppose at a pitchfork bifurcation point $\mu = \mu_0$, the solitary wave $u_0(\mathbf{x})$ is linearly stable (i.e., all its eigenvalues are either zero or purely imaginary); and when μ moves away from μ_0 , no complex eigenvalues bifurcate out from non-zero points on the imaginary axis. Then under the same conditions of Theorem 3, the base solution branch $u^0(\mathbf{x}; \mu)$ undergoes stability switching at the bifurcation point (with the right (left) side being unstable if the constant α in (3.8) is positive (negative)). Near the bifurcation point, the two bifurcated solution branches $u^\pm(\mathbf{x}; \mu)$ and the base solution branch (on the same side of the bifurcation point) have opposite (same) linear stability when their power slopes $P'_0(\mu_0)$ and $P'_\pm(\mu_0)$ have the same (opposite) sign.

Based on this theorem, there are eight possible types of pitchfork bifurcations in the GNLS equations (2.1), and their schematic solution-bifurcation diagrams (with stability information indicated) are displayed in Fig. 1. Here the four types in the upper (lower) row are when the bifurcation occurs for $\mu > \mu_0$ ($\mu < \mu_0$). The bifurcations in Fig. 1(a), (e) and (b), (f) are qualitatively the same as the supercritical and subcritical pitchfork bifurcations in finite-dimensional dynamical systems [18]. In these cases, the bifurcated solution branches and the base solution branch (on the same side of the bifurcation point) have opposite stability. The bifurcations in Fig. 1(c), (d), (g) and (h), however, are different. In these cases, the bifurcated solution branches and the base branch (on the same side of the bifurcation point) have the same stability (all stable or all unstable), which seems to have no counterpart in the finite-dimensional dynamical-system theory [18]. Note that the bifurcation in Fig. 1(c) has been reported in [8], but the bifurcations in Fig. 1(d), (g) and (h) have not been discovered before to the author's best knowledge.

Remark 3. In Theorem 4, the sign of α plays a critical role for the stability outcome. This sign can be determined as follows. From formula (3.8), we see that the sign of α is determined by the signs of R and $\langle \psi, L_{00}^{-1} \psi \rangle$. The sign of R can be read off from the shape of the power diagram. Specifically, we know from formula (2.10) that $P'_\pm(\mu_0) - P'_0(\mu_0)$ and S have the same sign. We also know from Theorem 1 that the side of $\mu = \mu_0$ to which the bifurcation occurs (left or right) determines the sign of the product RS (negative or positive). Thus using the sign of $P'_\pm(\mu_0) - P'_0(\mu_0)$ and the side of bifurcation from the power diagram, we can obtain the sign of R . The sign of α is then obtained accordingly. Specifically, the sign of α can be determined as follows.

- (i) If the bifurcation occurs for $\mu > \mu_0$, then the sign of α is equal to the sign of $\langle \psi, L_{00}^{-1} \psi \rangle$ multiplying the sign of $P'_\pm(\mu_0) - P'_0(\mu_0)$;
- (ii) If the bifurcation occurs for $\mu < \mu_0$, then the sign of α is opposite of the sign of $\langle \psi, L_{00}^{-1} \psi \rangle$ multiplying the sign of $P'_\pm(\mu_0) - P'_0(\mu_0)$.

After the sign of α is obtained, stability of all the solution branches can then be read off from the power diagram by Theorem 4. For instance, when $\langle \psi, L_{00}^{-1} \psi \rangle < 0$ and the bifurcation occurs for $\mu > \mu_0$, schematic power-stability diagrams of all six possible bifurcation scenarios are displayed in Fig. 2. This list of power-stability diagrams is compiled according to the signs of $P'_0(\mu_0)$, $P'_\pm(\mu_0)$, and $P'_\pm(\mu_0) - P'_0(\mu_0)$. If $\langle \psi, L_{00}^{-1} \psi \rangle < 0$ and the bifurcation occurs for $\mu < \mu_0$, schematic power-stability diagrams of all six possible bifurcation scenarios are displayed in Fig. 3. If $\langle \psi, L_{00}^{-1} \psi \rangle > 0$, these power diagrams remain the same, but the stability of all their solution branches is flipped

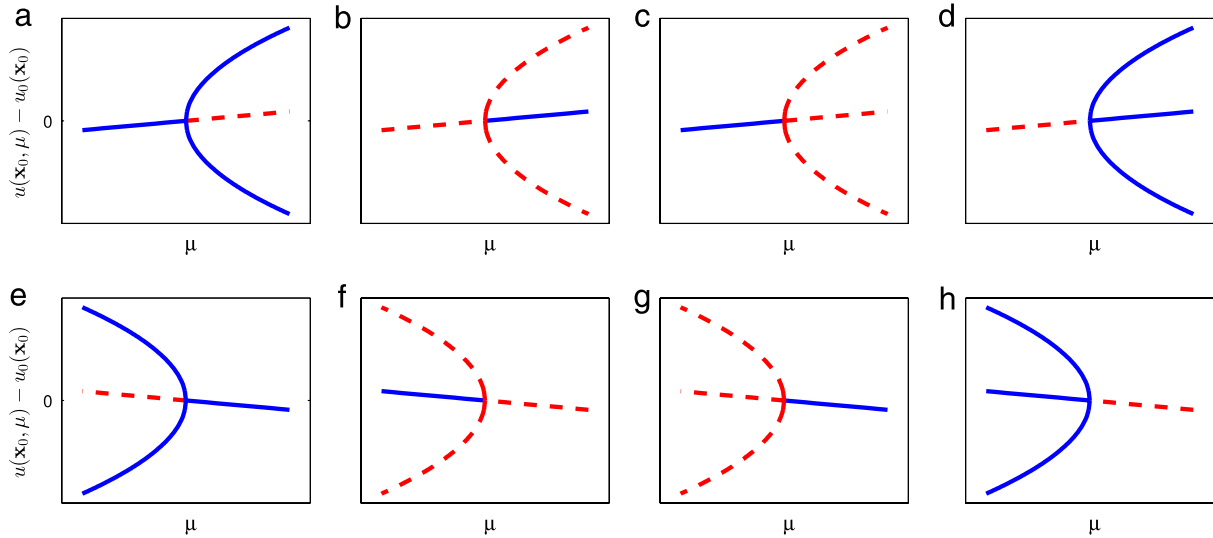


Fig. 1. (Color online) Schematic solution-bifurcation diagrams (with stability information indicated) for the eight types of pitchfork bifurcations in the GNLS equations (2.1). Plotted in this figure are deviations $u(\mathbf{x}_0; \mu) - u_0(\mathbf{x}_0)$ versus μ at a representative \mathbf{x}_0 position. Solid blue and dashed red lines represent stable and unstable branches respectively.

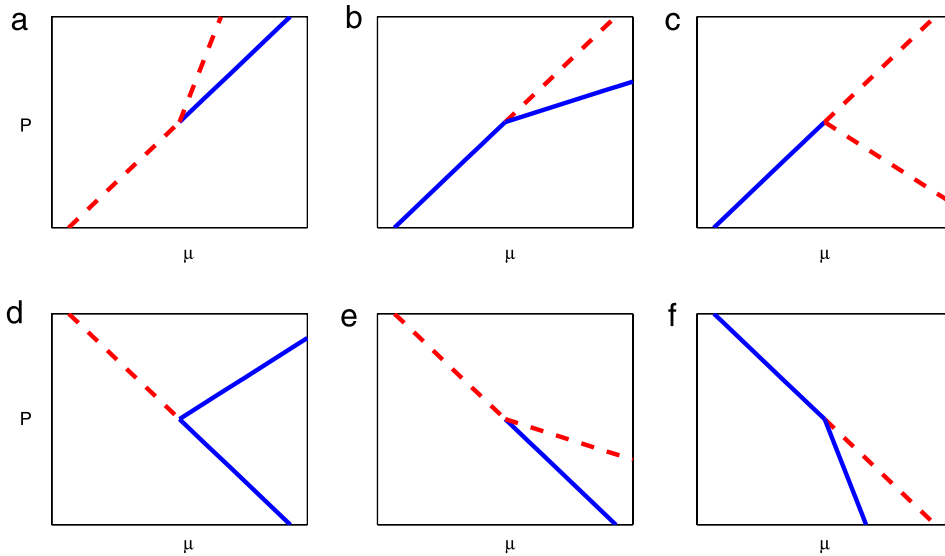


Fig. 2. (Color online) Six possible scenarios of the power-stability diagram for pitchfork bifurcations in the GNLS equations (2.1) when $\langle \psi, L_{00}^{-1} \psi \rangle < 0$ and the bifurcation occurs for $\mu > \mu_0$. Solid blue and dashed red lines indicate stable and unstable branches respectively. Since the two bifurcated solution branches $u^\pm(\mathbf{x}; \mu)$ have the same power slope at the bifurcation point (see Theorem 2), their power curves are shown by a single line in this schematic figure. If $\langle \psi, L_{00}^{-1} \psi \rangle > 0$, then the stability of every power branch is flipped.

(with “stable” changed to “unstable” and vice versa). These power-stability diagrams are useful for us to quickly predict linear stability from the power diagram.

One might notice that the power diagrams of pitchfork bifurcations in Figs. 2 and 3 split out to two rather than three branches at the bifurcation point, which is different from the solution-bifurcation diagrams in Fig. 1. The reason is that the two bifurcated solution branches $u^\pm(\mathbf{x}; \mu)$ have the same power slope at the bifurcation point (see Theorem 2), thus their power curves are drawn as the same line in these schematic power diagrams [11].

The above results (i.e., Theorems 1–4) are valid for all real-valued solitary waves $u(\mathbf{x}; \mu)$ in the GNLS equations (2.1), including both sign-definite (positive) and sign-indefinite (sign-changing) solitary waves. If the solitary waves are positive, then our stability results can be made stronger and more explicit. For positive solitary waves in Eq. (2.1), it is known that all eigenvalues in the linear-stability operator \mathcal{L} are either purely real

or purely imaginary (see Ref. [13, Theorem 5.2]). In addition, linear stability of the solitary wave $u_0(\mathbf{x})$ at the bifurcation point can be determined by the generalized Vakhitov–Kolokolov stability criterion (Ref. [13, Theorem 5.2]). Furthermore, zero is the largest eigenvalue of L_0 and is simple [27], and $\langle \psi, L_{00}^{-1} \psi \rangle < 0$ since operator L_{00} is semi-negative definite. Using this information, together with Theorem 4 and Remark 3, we can obtain the following stronger and more explicit theorem for the linear stability of positive solitary waves near a pitchfork bifurcation point. This theorem derives linear stability of these solitary waves almost exclusively from their power diagram.

Theorem 5. Suppose solitary waves in the GNLS equations (2.1) are positive near a pitchfork bifurcation point $\mu = \mu_0$. If $P'_0(\mu_0) < 0$ or L_{10} has more than one positive discrete eigenvalue, then solitary waves on both the base and bifurcated branches (near the bifurcation point) are linearly unstable. If $P'_0(\mu_0) > 0$, $P'_\pm(\mu_0) \neq 0$, and L_{10} has only

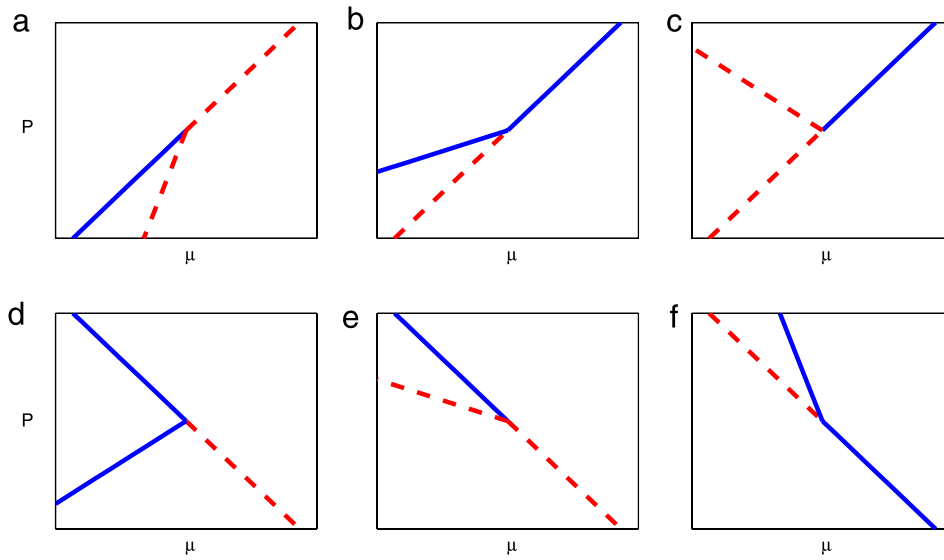


Fig. 3. (Color online) Six possible scenarios of the power-stability diagram for pitchfork bifurcations in the GNLS equations (2.1) when $\langle \psi, L_{00}^{-1} \psi \rangle < 0$ and the bifurcation occurs for $\mu < \mu_0$. Solid blue and dashed red lines indicate stable and unstable branches respectively. If $\langle \psi, L_{00}^{-1} \psi \rangle > 0$, then stability of every power branch is flipped.

one positive discrete eigenvalue and a simple discrete zero eigenvalue, then

- (1) when the bifurcation occurs for $\mu > \mu_0$ and $P'_{\pm}(\mu_0) < P'_0(\mu_0)$, the base solution branch $u^0(\mathbf{x}; \mu)$ is linearly stable for $\mu < \mu_0$ and unstable for $\mu > \mu_0$, whereas the bifurcated branches are linearly stable if $P'_{\pm}(\mu_0) > 0$ and unstable if $P'_{\pm}(\mu_0) < 0$;
- (2) when the bifurcation occurs for $\mu > \mu_0$ and $P'_{\pm}(\mu_0) > P'_0(\mu_0)$, the base solution branch is linearly unstable for $\mu < \mu_0$ and stable for $\mu > \mu_0$, whereas the bifurcated branches are always linearly unstable;
- (3) when the bifurcation occurs for $\mu < \mu_0$ and $P'_{\pm}(\mu_0) < P'_0(\mu_0)$, the base solution branch is linearly unstable for $\mu < \mu_0$ and stable for $\mu > \mu_0$, whereas the bifurcated branches are linearly stable if $P'_{\pm}(\mu_0) > 0$ and unstable if $P'_{\pm}(\mu_0) < 0$;
- (4) when the bifurcation occurs for $\mu < \mu_0$ and $P'_{\pm}(\mu_0) > P'_0(\mu_0)$, the base solution branch is linearly stable for $\mu < \mu_0$ and unstable for $\mu > \mu_0$, whereas the bifurcated branches are always linearly unstable.

In terms of solution-bifurcation diagrams, case (1) in this theorem belongs to pitchfork bifurcations of type (a) or (c) in Fig. 1, case (2) belongs to pitchfork bifurcations of type (b) in Fig. 1, case (3) belongs to pitchfork bifurcations of type (e) or (g) in Fig. 1, and case (4) belongs to pitchfork bifurcations of type (f) in Fig. 1. Thus for positive solitary waves in the GNLS equations (2.1), pitchfork bifurcations of type (d, h) in Fig. 1 cannot occur.

In terms of power-bifurcation diagrams, case (1) belongs to pitchfork bifurcations of type (b, c) in Fig. 2, case (2) belongs to pitchfork bifurcations of type (a) in Fig. 2, case (3) belongs to pitchfork bifurcations of type (b, c) in Fig. 3, and case (4) belongs to pitchfork bifurcations of type (a) in Fig. 3.

Remark 4. For positive solitary waves, pitchfork bifurcation cannot occur when L_{10} does not have any positive discrete eigenvalues (i.e., when zero is the largest discrete eigenvalue of L_{10}). The reason is that for any linear Schrödinger operator, the eigenfunction of its largest eigenvalue is always positive (sign-definite) [27]. Thus for this largest zero eigenvalue of L_{10} , its eigenfunction ψ is positive. Since $u_0(\mathbf{x})$ is also positive, then $\langle u_0, \psi \rangle \neq 0$, which violates the conditions of pitchfork bifurcations in Theorem 1. Thus this case is not mentioned in Theorem 5.

4. Connection with the Hamiltonian–Krein index theory

In recent years, a Hamiltonian–Krein index theory was developed for the qualitative study of linear stability of nonlinear waves in Hamiltonian systems [28–32]. Our linear-stability eigenvalue problem (2.12) can be rewritten as

$$\begin{bmatrix} 0 & 1 \\ -1 & 0 \end{bmatrix} \begin{bmatrix} -L_1 & 0 \\ 0 & -L_0 \end{bmatrix} \widehat{\Phi} = \lambda \widehat{\Phi}, \quad (4.1)$$

where $\widehat{\Phi} = [v, -iw]^T$, and the superscript ‘T’ represents the transpose of a vector. Denoting $p(\mathcal{A})$ as the number of positive eigenvalues in an operator \mathcal{A} and denoting $p(\alpha) = 1$ if a constant $\alpha > 0$ and $p(\alpha) = 0$ if $\alpha < 0$, then applying that index theory to this eigenvalue problem, we quickly get the following theorem.

Theorem 6. Near a pitchfork bifurcation point $\mu = \mu_0$ in Theorem 1, assume that the continuous spectra of L_0 and L_1 are negative and bounded away from zero. In addition, assume that L_0 and L_1 have a finite number of positive discrete eigenvalues (counting algebraic multiplicity). Then under the same assumptions and conditions in Theorem 3, the following Hamiltonian–Krein index formulae hold,

$$k_r + 2k_c + 2k_i = p(\mathcal{B}_1) + p(\mathcal{B}_0), \quad (4.2)$$

$$k_r \geq |p(\mathcal{B}_1) - p(\mathcal{B}_0)|. \quad (4.3)$$

Here k_r is the number of positive real eigenvalues in (4.1), k_c is the number of quadruplets of eigenvalues in (4.1) with nonzero real and imaginary parts, and k_i is the number of pairs of purely imaginary eigenvalues in (4.1) with negative Krein signature, counting their algebraic multiplicities. Operators \mathcal{B}_1 and \mathcal{B}_0 are defined as

$$\mathcal{B}_1 = L_1|_{\ker(L_0)^\perp}, \quad \mathcal{B}_0 = L_0|_{\ker(L_1)^\perp},$$

and $p(\mathcal{B}_1), p(\mathcal{B}_0)$ are given by the formulae

$$p(\mathcal{B}_1) = p(L_1) - \begin{cases} p(P'(\mu)), & \mu \neq \mu_0, \\ p(P'_0(\mu_0)), & \mu = \mu_0, \end{cases} \quad (4.4)$$

and

$$p(\mathcal{B}_0) = p(L_0) - \begin{cases} 0, & \mu \neq \mu_0, \\ p(\langle \psi, L_{00}^{-1} \psi \rangle), & \mu = \mu_0. \end{cases} \quad (4.5)$$

Remark 5. Obviously $p(\mathcal{B}_1)$ and $p(\mathcal{B}_0)$ must be nonnegative.

Remark 6. In the index theory, the quantity subtracted on the right side of Eq. (4.4) is originally $p(\langle u, L_1^{-1}u \rangle)$. When $\mu \neq \mu_0$, we see from Eq. (2.17) that $L_1^{-1}u = u_\mu$, thus $p(\langle u, L_1^{-1}u \rangle) = p(P'(\mu))$. When $\mu = \mu_0$, we see from Eq. (2.9) that $p(\langle u_0, L_{10}^{-1}u_0 \rangle) = p(P'_0(\mu_0))$. Thus we obtain the more explicit formula (4.4).

Remark 7. According to the assumption in Theorem 3, zero is a simple discrete eigenvalue of L_{10} with eigenfunction ψ at $\mu = \mu_0$, thus $p(\langle \psi, L_{00}^{-1}\psi \rangle)$ needs to be subtracted in the formula (4.5). When $\mu \neq \mu_0$, under the conditions of pitchfork bifurcations in Theorem 1, this zero eigenvalue in L_1 bifurcates out (see Lemma 1 below), thus the kernel of L_1 is empty, which means that $\mathcal{B}_0 = L_0$ and $p(\mathcal{B}_0) = p(L_0)$.

Remark 8. One of the main assumptions in Theorem 6 is that the continuous spectra of L_0 and L_1 are negative and the number of their positive eigenvalues is finite. This means that Theorem 6 does not apply to gap solitons in the GNLS equations (2.1), which exist inside a gap between two continuous-spectrum bands. Our Theorems 3 and 4, however, apply to all solitons including gap solitons.

In order to use Theorem 6, we need to know $p(L_0)$ and $p(L_1)$. A way to get $p(L_0)$ is the following. Under the assumption in Theorem 3, zero is a simple discrete eigenvalue of L_{00} . Since this zero eigenvalue persists in L_0 when $\mu \neq \mu_0$ (see (2.16)), we find that

$$p(L_0) = p(L_{00}), \quad |\mu - \mu_0| \ll 1.$$

To get $p(L_{00})$, we notice that for the stability analysis of pitchfork bifurcations to be meaningful, the solitary wave $u_0(\mathbf{x})$ at the bifurcation point $\mu = \mu_0$ should be linearly stable (see assumptions in Theorem 4). Then in view of Eq. (4.3), it should be minimally true that $p(\mathcal{B}_1) = p(\mathcal{B}_0)$ at $\mu = \mu_0$. Using the formulae (4.4)–(4.5), we then get

$$p(L_{00}) = p(L_{10}) - p(P'_0(\mu_0)) + p(\langle \psi, L_{00}^{-1}\psi \rangle).$$

Since $P'_0(\mu_0) \neq 0$ due to conditions (3.6), and since $P'_0(\mu)$ is a continuous function of μ , we see that $p(P'_0(\mu)) = p(P'_0(\mu_0))$ near the pitchfork bifurcation point. Thus when $|\mu - \mu_0| \ll 1$,

$$p(L_0) = p(L_{10}) - p(P'_0(\mu)) + p(\langle \psi, L_{00}^{-1}\psi \rangle). \quad (4.6)$$

To get $p(L_1)$, we need to know in which direction the simple zero eigenvalue of L_{10} bifurcates out when $\mu \neq \mu_0$. The answer to this question is given by the following lemma.

Lemma 1. Suppose $\Lambda_0(\mu)$ and $\Lambda_\pm(\mu)$ are discrete eigenvalues of L_1 on the base and bifurcated solution branches $u^0(\mathbf{x}; \mu)$ and $u^\pm(\mathbf{x}; \mu)$, with $\Lambda_0(\mu_0) = \Lambda_\pm(\mu_0) = 0$ at the bifurcation point $\mu = \mu_0$. Then under the conditions for pitchfork bifurcations in Theorem 1, we have

$$\Lambda'_0(\mu_0) = -\frac{R}{\langle \psi, \psi \rangle}, \quad (4.7)$$

and

$$\Lambda'_+(\mu_0) = \Lambda'_-(\mu_0) = -2\Lambda'_0(\mu_0). \quad (4.8)$$

The proof of this lemma is given in the end of the next section.

Remark 9. This lemma shows that under the conditions of pitchfork bifurcations (where $R \neq 0$, see Theorem 1), the zero eigenvalue in L_1 always bifurcates out on both the base and bifurcated solution branches when $\mu \neq \mu_0$, because $\Lambda'_0(\mu_0)$ and $\Lambda'_\pm(\mu_0)$ are nonzero. In addition, these eigenvalue bifurcations on the base and bifurcated branches are always along opposite directions since $\Lambda'_0(\mu_0)$ and $\Lambda'_\pm(\mu_0)$ have opposite signs. Furthermore, directions

of these eigenvalue bifurcations are uniquely determined by the sign of R . Recall from Theorem 1 and Eq. (2.10) that the sign of R is uniquely determined by the sign of $P'_\pm(\mu_0) - P'_0(\mu_0)$ and to which side of $\mu = \mu_0$ the bifurcation occurs (see also Remark 3). Thus directions of eigenvalue bifurcations in L_1 are uniquely determined by the shape of the power diagram. This fact, together with the index formulae (4.2)–(4.3), clearly signals that the shape of the power diagram plays a decisive role in the stability outcome, which was the main theme of the previous section.

Using the formula (4.6) and defining the total Hamiltonian–Krein index

$$K_T \equiv k_r + 2k_c + 2k_i, \quad (4.9)$$

the index formula (4.2) for the base solution branch and $\mu \neq \mu_0$ then reduces to

$$K_T^0 = p(L_1^0) + p(L_{10}) - 2p(P'_0(\mu)) + p(\langle \psi, L_{00}^{-1}\psi \rangle). \quad (4.10)$$

Here the superscript ‘0’ in K_T^0 and L_1^0 indicates that these quantities are for the base-solution branch. For the bifurcated solution branches, this index formula for $\mu \neq \mu_0$ reduces to

$$K_T^\pm = p(L_1^\pm) + p(L_{10}) - p(P'_0(\mu)) - p(P'_\pm(\mu)) + p(\langle \psi, L_{00}^{-1}\psi \rangle). \quad (4.11)$$

Here the superscript ‘ \pm ’ in K_T^\pm and L_1^\pm indicates that these quantities are for the bifurcated solution branches. These formulae, together with Lemma 1 (which provides information on $p(L_1^0)$ and $p(L_1^\pm)$), then allow us to calculate the Hamiltonian–Krein index.

Below we show that, if the assumptions of Theorem 6 are met, then the above index theory can reproduce the qualitative stability results obtained in the previous section (except Theorem 3). Re-derivation of Theorem 4 will be explained in detail, but re-derivation of Theorem 5 will be omitted for brevity.

First we consider the base solution branch. On the two sides of $\mu = \mu_0$ of this branch, $p(L_1^0)$ differs by one in view of Lemma 1, while the other indices on the right hand side of Eq. (4.10) do not change (when μ is near μ_0). Thus the total Hamiltonian–Krein index K_T^0 is odd on one side of $\mu = \mu_0$ and even on the other side of $\mu = \mu_0$. On the side of odd K_T^0 , there is at least one real positive eigenvalue due to the definition (4.9), thus the base solitary wave is unstable. Under the assumptions of Theorem 4 where the solitary wave $u_0(\mathbf{x})$ is stable at the bifurcation point and no complex eigenvalues appear when $\mu \neq \mu_0$, we see that there is a single positive eigenvalue on the side of odd K_T^0 and no unstable eigenvalues on the side of even K_T^0 , thus stability switches at $\mu = \mu_0$ on the base branch, in agreement with Theorem 4.

Now we consider the bifurcated branches. The index $p(L_1^\pm)$ on these branches and $p(L_1^0)$ on the base branch differ by one in view of Lemma 1. Thus if $P'_0(\mu)$ and $P'_\pm(\mu)$ have the same sign, then due to formulae (4.10) and (4.11), one of K_T^0 and K_T^\pm would be even and the other one odd. Thus under the assumptions of Theorem 4, the base and bifurcated branches would have opposite linear stability. On the other hand, if $P'_0(\mu)$ and $P'_\pm(\mu)$ have the opposite sign, then K_T^0 and K_T^\pm would be both even or both odd. Under the assumptions of Theorem 4, the base and bifurcated branches would have the same linear stability. Again, these results agree with Theorem 4.

More specific stability results in Theorem 4 (based on the sign of α) can also be reproduced by the index theory. Since these specific stability results are summarized in Figs. 2 and 3 for $\langle \psi, L_{00}^{-1}\psi \rangle < 0$ (stability of every branch would flip when $\langle \psi, L_{00}^{-1}\psi \rangle > 0$), we will rederive some of these specific stability results in these figures as examples below.

- (1) Consider Fig. 2(a). In this case, $\langle \psi, L_{00}^{-1} \psi \rangle < 0$, the bifurcation occurs for $\mu > \mu_0$, and $P'_\pm(\mu) > P'_0(\mu) > 0$. From Theorems 1 and 2, we see that $S > 0$ and $RS > 0$, thus $R > 0$. Lemma 1 then shows that $p(L_1^0)$ for $\mu < \mu_0$ is one more than that for $\mu \geq \mu_0$. Suppose

$$p(L_1^0) = \begin{cases} k + 1, & \mu < \mu_0, \\ k, & \mu \geq \mu_0, \end{cases} \quad (4.12)$$

where k is some nonnegative integer. Then in view of Lemma 1,

$$p(L_1^\pm) = k + 1, \quad \mu > \mu_0. \quad (4.13)$$

Thus from formulae (4.10) and (4.11), we get

$$K_T^0 = \begin{cases} 2k - 1, & \mu < \mu_0, \\ 2k - 2, & \mu > \mu_0, \end{cases}$$

and

$$K_T^\pm = 2k - 1, \quad \mu > \mu_0.$$

This means that $k \geq 1$. In addition, the base branch for $\mu < \mu_0$ and the bifurcated branches have at least one positive eigenvalue, but the base branch for $\mu > \mu_0$ could be stable. Under the assumptions of Theorem 4, the base branch for $\mu < \mu_0$ and the bifurcated branches are then linearly unstable and the base branch for $\mu \geq \mu_0$ is stable, in agreement with the stability result in Fig. 2(a).

- (2) Consider Fig. 2(d). In this case, $\langle \psi, L_{00}^{-1} \psi \rangle < 0$, the bifurcation occurs for $\mu > \mu_0$, $P'_0(\mu) < 0$, and $P'_\pm(\mu) > 0$. From Theorems 1 and 2, we get $R > 0$. Then according to Lemma 1, $p(L_1^0)$ and $p(L_1^\pm)$ are as given in (4.12) and (4.13). Thus we get from formulae (4.10) and (4.11) that

$$K_T^0 = \begin{cases} 2k + 1, & \mu < \mu_0, \\ 2k, & \mu > \mu_0, \end{cases}$$

and

$$K_T^\pm = 2k, \quad \mu > \mu_0.$$

This means that the base branch for $\mu < \mu_0$ has at least one positive eigenvalue. Under the assumptions of Theorem 4, the base branch for $\mu < \mu_0$ is then linearly unstable, and the base branch for $\mu \geq \mu_0$ as well as the bifurcated branches is stable, in agreement with the stability result in Fig. 2(d).

- (3) Consider Fig. 3(c). In this case, $\langle \psi, L_{00}^{-1} \psi \rangle < 0$, the bifurcation occurs for $\mu < \mu_0$, $P'_0(\mu) > 0$, and $P'_\pm(\mu) < 0$. From Theorems 1 and 2, we see that $S < 0$ and $RS < 0$, thus $R > 0$. Then according to Lemma 1, $p(L_1^0)$ and $p(L_1^\pm)$ are as given in (4.12) and (4.13). Thus we get from formulae (4.10) and (4.11) that

$$K_T^0 = \begin{cases} 2k - 1, & \mu < \mu_0, \\ 2k - 2, & \mu > \mu_0, \end{cases}$$

and

$$K_T^\pm = 2k - 1, \quad \mu < \mu_0.$$

This means that $k \geq 1$. In addition, the base branch for $\mu < \mu_0$ and the bifurcated branches have at least one positive eigenvalue, but the base branch for $\mu > \mu_0$ could be stable. Under the assumptions of Theorem 4, the base branch for $\mu < \mu_0$ and the bifurcated branches are then linearly unstable and the base branch for $\mu \geq \mu_0$ is stable, in agreement with the stability result in Fig. 3(c).

- (4) Consider Fig. 3(d). In this case, $\langle \psi, L_{00}^{-1} \psi \rangle < 0$, the bifurcation occurs for $\mu < \mu_0$, $P'_0(\mu) < 0$, and $P'_\pm(\mu) > 0$. From Theorems 1 and 2, we see that $S > 0$ and $RS < 0$, thus $R < 0$. Then according to Lemma 1, $p(L_1^0)$ and $p(L_1^\pm)$ become

$$p(L_1^0) = \begin{cases} k, & \mu \leq \mu_0, \\ k + 1, & \mu > \mu_0, \end{cases}$$

and

$$p(L_1^\pm) = k + 1, \quad \mu < \mu_0,$$

where k is some nonnegative integer. Thus we get from formulae (4.10) and (4.11) that

$$K_T^0 = \begin{cases} 2k, & \mu < \mu_0, \\ 2k + 1, & \mu > \mu_0, \end{cases}$$

and

$$K_T^\pm = 2k, \quad \mu < \mu_0.$$

This means that the base branch for $\mu > \mu_0$ has at least one positive eigenvalue. Under the assumptions of Theorem 4, the base branch for $\mu > \mu_0$ is then linearly unstable, and the base branch for $\mu \leq \mu_0$ as well as the bifurcated branches is stable, in agreement with the stability result in Fig. 3(d).

When $\langle \psi, L_{00}^{-1} \psi \rangle > 0$, the total Hamiltonian–Krein indices K_T for the power diagrams in Figs. 2 and 3 are simply those of $\langle \psi, L_{00}^{-1} \psi \rangle < 0$ plus one (see formulae (4.10) and (4.11)). Thus under the assumptions of Theorem 4, linear stability of all branches in Figs. 2 and 3 is flipped, in agreement with the results in the previous section.

It is important to notice that in order for a solution branch to be stable when $\langle \psi, L_{00}^{-1} \psi \rangle > 0$, the total Hamiltonian–Krein index K_T for $\langle \psi, L_{00}^{-1} \psi \rangle < 0$ needs to be odd, hence $K_T \geq 2$ for $\langle \psi, L_{00}^{-1} \psi \rangle > 0$. This means that

if $\langle \psi, L_{00}^{-1} \psi \rangle > 0$, every stable solitary wave must possess imaginary eigenvalues of negative Krein signature.

The index theory can also yield other useful information. For instance, from Eq. (4.4) and Remark 5, we have that

$$\text{if } p(L_{10}) = 0, \text{ then } P'_0(\mu_0) < 0.$$

That is, if the largest eigenvalue of L_1 crosses zero at $\mu = \mu_0$, then the slope of the base branch's power curve at $\mu = \mu_0$ must be negative.

It should be cautioned, however, that all these results from the index theory were derived under the spectral assumptions that the continuous spectra of L_0 and L_1 are negative and the number of their positive eigenvalues is finite. These assumptions are not needed for Theorems 4 and 5.

5. Proofs of the main results

Proof of Theorem 3. The basic idea of the proof is that we first show the algebraic multiplicity of the zero eigenvalue in the linear-stability operator \mathcal{L} is four at the bifurcation point $\mu = \mu_0$ and drops to two away from it, thus a pair of eigenvalues bifurcate out from the origin when $\mu \neq \mu_0$. This pair of eigenvalues must bifurcate along the real or imaginary axis since eigenvalues of \mathcal{L} would appear as quadruples if this bifurcation were not along these two axes. Then we calculate this pair of eigenvalues near the bifurcation point $\mu = \mu_0$ by perturbation methods. We show that the perturbation series for these bifurcated eigenvalues can be constructed to all orders, with the leading-order terms given by Eqs. (3.7) and (3.9) for solitary waves on the base and bifurcated branches respectively.

At the pitchfork bifurcation point $\mu = \mu_0$ in Theorem 1, $(0, u_0)^T$ and $(\psi, 0)^T$ are eigenfunctions of the zero eigenvalue in \mathcal{L}_0 in view of Eq. (3.5). Under the assumption in Theorem 3, \mathcal{L}_0 does not admit any additional eigenfunctions at the zero eigenvalue, thus the geometric multiplicity of this zero eigenvalue is two. Next we determine the algebraic multiplicity of this zero eigenvalue by examining its generalized eigenfunctions.

First, evaluating the relation (2.17) along the base solution branch $u^0(\mathbf{x}; \mu)$ at $\mu = \mu_0$, we get

$$L_{10}u_{\mu_0}^0 = u_0,$$

where $u_{\mu_0}^0$ is equal to u_{μ}^0 evaluated at $\mu = \mu_0$. Thus,

$$\mathcal{L}_0 \begin{bmatrix} u_{\mu_0}^0 \\ 0 \end{bmatrix} = \begin{bmatrix} 0 \\ u_0 \end{bmatrix},$$

which means that $(u_{\mu_0}^0, 0)^T$ is a generalized eigenfunction of the zero eigenvalue. The next-order generalized eigenfunction $(f_2, g_2)^T$ satisfies the equation

$$\mathcal{L}_0 \begin{bmatrix} f_2 \\ g_2 \end{bmatrix} = \begin{bmatrix} u_{\mu_0}^0 \\ 0 \end{bmatrix},$$

so the equation for g_2 is

$$L_{00}g_2 = u_{\mu_0}^0. \quad (5.1)$$

Since u_0 is a homogeneous solution of this equation, L_{00} is self-adjoint, and $\langle u_0, u_{\mu_0}^0 \rangle = P'_0(\mu_0)/2 \neq 0$ by conditions (3.6), according to the Fredholm alternative theorem, Eq. (5.1) does not admit localized solutions for g_2 , thus there are no additional generalized eigenfunctions for $(0, u_0)^T$.

Next, we consider generalized eigenfunctions of \mathcal{L}_0 for $(\psi, 0)^T$. The lowest-order generalized eigenfunction $(f_1, g_1)^T$ satisfies the equation

$$\mathcal{L}_0 \begin{bmatrix} f_1 \\ g_1 \end{bmatrix} = \begin{bmatrix} \psi \\ 0 \end{bmatrix}.$$

According to the assumption in Theorem 3, the kernel of L_{00} contains a single localized function u_0 , and $\langle u_0, \psi \rangle = 0$ in view of the conditions for pitchfork bifurcations in Theorem 1. Thus from the Fredholm alternative theorem, there exists a real localized function $L_{00}^{-1}\psi$. Consequently,

$$\mathcal{L}_0 \begin{bmatrix} 0 \\ L_{00}^{-1}\psi \end{bmatrix} = \begin{bmatrix} \psi \\ 0 \end{bmatrix},$$

i.e., $(0, L_{00}^{-1}\psi)^T$ is a generalized eigenfunction of \mathcal{L}_0 . The next-order generalized eigenfunction $(f_2, g_2)^T$ for $(\psi, 0)^T$ satisfies the equation

$$\mathcal{L}_0 \begin{bmatrix} f_2 \\ g_2 \end{bmatrix} = \begin{bmatrix} 0 \\ L_{00}^{-1}\psi \end{bmatrix},$$

so the equation for f_2 is

$$L_{10}f_2 = L_{00}^{-1}\psi. \quad (5.2)$$

Since ψ is a homogeneous solution of this equation and $\langle \psi, L_{00}^{-1}\psi \rangle \neq 0$ by conditions (3.6), Eq. (5.2) does not admit any localized solutions by the Fredholm alternative theorem. Thus there are no additional generalized eigenfunctions for $(\psi, 0)^T$.

The above analysis shows that \mathcal{L}_0 has two eigenfunctions and two generalized eigenfunctions at the zero eigenvalue, thus the algebraic multiplicity of the zero eigenvalue in \mathcal{L}_0 (at the bifurcation point) is four.

When $0 < |\mu - \mu_0| \ll 1$, on any solitary-wave branch $u^0(\mathbf{x}; \mu)$ or $u^{\pm}(\mathbf{x}; \mu)$, Eq. (2.16) still holds. Thus due to assumptions in Theorem 3, zero is still a simple eigenvalue of L_0 . Using perturbation analysis, we can also show that, under the conditions of pitchfork bifurcations in Theorem 1 and assumptions in Theorem 3, zero is not an eigenvalue of L_1 anymore (see Lemma 1 in Section 4). From these facts, we see that when $0 < |\mu - \mu_0| \ll 1$, zero is an eigenvalue of \mathcal{L} with geometric multiplicity one, and its eigenfunction is $(0, u)^T$. Regarding the algebraic multiplicity of this zero eigenvalue in \mathcal{L} , we recall that for $\mu \neq \mu_0$, Eq. (2.17) still holds. Thus it is easy to see that $(u_{\mu}, 0)^T$ is a generalized eigenfunction of this zero eigenvalue. Due to conditions (3.6) in Theorem 3 and smoothness of the power functions (see the note below Theorem 1), we see

that $P'_0(\mu) \neq 0$ and $P'_{\pm}(\mu) \neq 0$ when $0 < |\mu - \mu_0| \ll 1$. Then by similar analysis as above, we can show that the zero eigenvalue in \mathcal{L} does not admit any additional generalized eigenfunctions. Thus when $0 < |\mu - \mu_0| \ll 1$, the algebraic multiplicity of this zero eigenvalue in \mathcal{L} is two.

Since the algebraic multiplicity of the zero eigenvalue in \mathcal{L} is four at $\mu = \mu_0$ and drops to two when $\mu \neq \mu_0$, this means that when μ moves away from μ_0 , a pair of linear-stability eigenvalues must bifurcate out from the origin. Notice that the two multiplicities of the zero eigenvalue associated with the phase-invariance mode (2.18) persist when $\mu \neq \mu_0$ (see above), it is then clear that the two non-zero eigenvalues must bifurcate out from the bifurcation-induced zero eigenmode (3.2). Since eigenvalues of the linear-stability operator \mathcal{L} always appear in quadruples (when they are complex) or in pairs (when they are real or purely imaginary) (see discussions below Eq. (2.15)), this bifurcated pair of eigenvalues then must be real or purely imaginary and be opposite of each other as a $\pm\lambda$ pair.

Next, we calculate this pair of bifurcated eigenvalues on the solution branches $u^0(\mathbf{x}; \mu)$ and $u^{\pm}(\mathbf{x}; \mu)$. Since at the bifurcation point the zero eigenvalue of \mathcal{L}_0 is not embedded inside \mathcal{L}_0 's continuous spectrum, this allows us to calculate this eigenvalue bifurcation by the perturbation methods (see Remark 1). Justification on the use of perturbation series for eigenvalue calculations can be found in [33].

(a) *Eigenvalue bifurcation along the base solution branch*

We first calculate this eigenvalue bifurcation along the base solution branch $u^0(\mathbf{x}; \mu)$. These solitary waves near the bifurcation point $\mu = \mu_0$ have the following perturbation series expansion

$$u^0(\mathbf{x}; \mu) = \sum_{k=0}^{\infty} (\mu - \mu_0)^k u_k(\mathbf{x}), \quad (5.3)$$

where u_1, u_2, \dots are all real functions [11]. As a consequence, operators L_0 and L_1 on this base solution branch can be expanded as

$$L_0^0 = \sum_{k=0}^{\infty} (\mu - \mu_0)^k L_{0k}, \quad L_1^0 = \sum_{k=0}^{\infty} (\mu - \mu_0)^k L_{1k}. \quad (5.4)$$

The linear-stability eigenmodes (v, w, λ) bifurcated from the zero eigenmode (3.2) have the following perturbation series expansions:

$$v^0(\mathbf{x}; \mu) = \sum_{k=0}^{\infty} (\mu - \mu_0)^k v_k(\mathbf{x}), \quad (5.5)$$

$$w^0(\mathbf{x}; \mu) = \lambda_0(\mu - \mu_0)^{1/2} \sum_{k=0}^{\infty} (\mu - \mu_0)^k w_k(\mathbf{x}), \quad (5.6)$$

$$\lambda^0(\mu) = i\lambda_0(\mu - \mu_0)^{1/2} \left(1 + \sum_{k=1}^{\infty} (\mu - \mu_0)^k \lambda_k \right). \quad (5.7)$$

Below we construct these perturbation series solutions to all orders, and show that the leading-order expressions for the bifurcated eigenvalues $\lambda^0(\mu)$ are given by the formula (3.7).

We start by substituting the above perturbation expansions into the linear-stability eigenvalue problem (2.15). From these equations at various orders of $\mu - \mu_0$, we get a sequence of linear equations for (v_k, w_k) :

$$L_{10}v_0 = 0, \quad (5.8)$$

$$L_{00}w_0 = v_0, \quad (5.9)$$

$$L_{10}v_1 = \lambda_0^2 w_0 - L_{11}v_0, \quad (5.10)$$

$$L_{00}w_1 = v_1 + \lambda_1 w_0 - L_{01}w_0, \quad (5.11)$$

$$L_{10}v_2 = \lambda_0^2 (w_1 + \lambda_1 w_0) - (L_{11}v_1 + L_{12}v_0), \quad (5.12)$$

$$L_{00}w_2 = v_2 + \lambda_1 v_1 + \lambda_2 v_0 - (L_{01}w_1 + L_{02}w_0), \tag{5.13}$$

.....

$$L_{10}v_{n+1} = \lambda_0^2 \left(w_n + \sum_{k=1}^n \lambda_k w_{n-k} \right) - \sum_{k=1}^{n+1} L_{1k}v_{n+1-k}, \tag{5.14}$$

$$L_{00}w_{n+1} = v_{n+1} + \sum_{k=1}^{n+1} \lambda_k v_{n+1-k} - \sum_{k=1}^{n+1} L_{0k}w_{n+1-k}, \tag{5.15}$$

.....

All these equations are inhomogeneous except the first equation for v_0 . From the assumption in Theorem 3, the v_n equations have a single homogeneous solution ψ , and the w_n equations have a single homogeneous solution u_0 . Since operators L_{00} and L_{10} in these equations are self-adjoint, the Fredholm alternative theorem says that the inhomogeneous equations above are solvable if and only if their right hand sides are orthogonal to their homogeneous solution. These orthogonality conditions, together with a scaling of the eigenfunction (v, w) , will determine the eigenvalue coefficients λ_n as well as functions (v_n, w_n) for all $n \geq 0$, as will be demonstrated below.

First we consider the v_0 Eq. (5.8). In view of the assumption in Theorem 3, the only solution to this equation (after eigenfunction scaling) is

$$v_0 = \psi. \tag{5.16}$$

For the w_0 Eq. (5.9), due to the condition of $\langle u_0, \psi \rangle = 0$ for pitchfork bifurcations in Theorem 1, the Fredholm condition is satisfied, thus this equation admits a real localized solution $L_{00}^{-1}\psi$, and its general solution is

$$w_0 = L_{00}^{-1}\psi + c_0 u_0, \tag{5.17}$$

where c_0 is a constant to be determined from the solvability condition of the w_1 equation later.

For the v_1 Eq. (5.10), it is solvable if and only if its right hand side is orthogonal to ψ . Utilizing the v_0 and w_0 solutions derived above, this orthogonality condition yields the formula for the eigenvalue coefficient λ_0 as

$$\lambda_0^2 = \frac{\langle \psi, L_{11}\psi \rangle}{\langle \psi, L_{00}^{-1}\psi \rangle}. \tag{5.18}$$

According to our conditions (3.6), the denominator in the above formula is non-zero, thus λ_0^2 is well defined and is real. Later in this proof, we will derive a more explicit expression for λ_0^2 and show that it is non-zero as well (see Eq. (5.29)). The above Eq. (5.18) gives two real or purely imaginary λ_0 values as a ‘ \pm ’ pair.

With the eigenvalue coefficient λ_0 given in (5.18), the orthogonality condition of the v_1 Eq. (5.10) is satisfied, thus the general solution for v_1 is

$$v_1 = \widehat{v}_1 + \lambda_0^2 c_0 L_{10}^{-1}u_0 + d_1 \psi, \tag{5.19}$$

where \widehat{v}_1 is a real and localized particular solution to the v_1 Eq. (5.10) but without the c_0 term in w_0 on its right hand side (see (5.17)). This c_0 term induces its own particular solution in v_1 , which is the middle term in (5.19). In this term, $L_{10}^{-1}u_0$ is a real localized function which exists since u_0 is orthogonal to the function ψ in the kernel of L_{10} . The last term in (5.19) is the homogeneous solution, where d_1 is a free real constant. Since this homogeneous term in v_1 can be lumped to the v_0 term as $v_0 = [1 + d_1(\mu - \mu_0)]\psi$ and then eliminated by a scaling of the eigenfunction (v, w) , we will set $d_1 = 0$. A similar treatment will be applied to all higher v_n solutions.

Now we consider the w_1 Eq. (5.11). Its solvability condition is that its right hand side be orthogonal to the homogeneous solution

u_0 . Noticing that v_0 is orthogonal to u_0 and L_{01} is a real function, this solvability condition then reduces to

$$\langle u_0, v_1 \rangle - \langle L_{01}u_0, w_0 \rangle = 0. \tag{5.20}$$

To simplify this condition, we recall the relation $L_0 u^0(\mathbf{x}; \mu) = 0$. By inserting the expansions (5.3) and (5.4) for L_0 and $u^0(\mathbf{x}; \mu)$ into this relation and collecting terms of $O(\mu - \mu_0)$, we get

$$L_{01}u_0 = -L_{00}u_1. \tag{5.21}$$

When this relation and the solutions of w_0 and v_1 are substituted into the solvability condition (5.20) and after simple algebra, this solvability condition then reduces to

$$c_0 \lambda_0^2 \langle u_0, L_{10}^{-1}u_0 \rangle = -\langle u_0, \widehat{v}_1 \rangle - \langle u_1, \psi \rangle. \tag{5.22}$$

From Eq. (2.9) and conditions (3.6), $\langle u_0, L_{10}^{-1}u_0 \rangle \neq 0$. In addition, we will see from Eq. (5.29) later that $\lambda_0^2 \neq 0$ as well. Thus the solvability condition (5.22) yields a unique real value for c_0 as

$$c_0 = -\frac{\langle u_0, \widehat{v}_1 \rangle + \langle u_1, \psi \rangle}{\lambda_0^2 \langle u_0, L_{10}^{-1}u_0 \rangle}.$$

Consequently, the w_0 and v_1 solutions are now fully determined and are both real. In addition, with this c_0 value, the w_1 Eq. (5.11) is solvable, and its solution is

$$w_1 = \widehat{w}_1 + \lambda_1 L_{00}^{-1}\psi + c_1 u_0, \tag{5.23}$$

where \widehat{w}_1 is a real and localized particular solution to the w_1 Eq. (5.11) but without the λ_1 term on its right hand side, and c_1 is a constant. The eigenvalue coefficient λ_1 and the constant c_1 will be determined from the solvability conditions of the v_2 and w_2 Eqs. (5.12)–(5.13).

Next we use the method of induction to show that all higher-order terms in the perturbation series expansions (5.5)–(5.7) of (v, w, λ) can be successively determined and are all real-valued. Suppose the v_0, v_1, \dots, v_n and w_0, w_1, \dots, w_{n-1} solutions as well as $\lambda_1, \lambda_2, \dots, \lambda_{n-1}$ have been fully obtained and are all real. In addition, suppose the v_n solution is of the form

$$v_n = \widehat{v}_n + \lambda_0^2 c_{n-1} L_{10}^{-1}u_0, \tag{5.24}$$

where \widehat{v}_n is a real and localized function, and c_{n-1} is a real constant. Furthermore, suppose the w_n solution is of the form

$$w_n = \widehat{w}_n + \lambda_n L_{00}^{-1}\psi + c_n u_0, \tag{5.25}$$

where \widehat{w}_n is a known real and localized function but the coefficients λ_n and c_n are not known yet. These assumptions are satisfied when $n = 1$ (see above). We now show if they hold for n then they would still hold for $n + 1$ as well.

To determine λ_n , we use the solvability condition of the v_{n+1} Eq. (5.14). Inserting (5.25) into this solvability condition and utilizing (5.17), we readily find that

$$\lambda_n = \frac{\left\langle \psi, \sum_{k=1}^{n+1} L_{1k}v_{n+1-k} \right\rangle - \lambda_0^2 \left\langle \psi, \widehat{w}_n + \sum_{k=1}^{n-1} \lambda_k w_{n-k} \right\rangle}{2\lambda_0^2 \langle \psi, L_{00}^{-1}\psi \rangle},$$

which is real. For this λ_n value, the v_{n+1} Eq. (5.14) is solvable, and its solution is of the form

$$v_{n+1} = \widehat{v}_{n+1} + \lambda_0^2 c_n L_{10}^{-1}u_0,$$

where \widehat{v}_{n+1} is a real and localized particular solution to the v_{n+1} equation but without the c_n term in w_n on its right hand side (see (5.25)). Notice that this v_{n+1} solution is of the same form as v_n in (5.24) but with the index n changed to $n + 1$.

To determine the constant c_n in the above w_n and v_{n+1} solutions, we use the solvability condition of the w_{n+1} Eq. (5.15), which is that

its right hand side be orthogonal to the homogeneous solution u_0 . Inserting the above w_n and v_{n+1} solutions into this solvability condition and utilizing the relation (5.21), we find that this solvability condition yields the c_n value as

$$c_n = \frac{1}{\lambda_0^2 \langle u_0, L_{10}^{-1} u_0 \rangle} \left[\left\langle u_0, L_{01} \widehat{w}_n + \sum_{k=2}^{n+1} L_{0k} w_{n+1-k} \right\rangle - \left\langle u_0, \widehat{v}_{n+1} + \sum_{k=1}^n \lambda_k v_{n+1-k} \right\rangle - \lambda_n \langle u_1, \psi \rangle \right],$$

which is a real constant. With this c_n value, the w_n and v_{n+1} solutions are now fully determined and are both real. In addition, the w_{n+1} Eq. (5.15) is now solvable, and its general solution is

$$w_{n+1} = \widehat{w}_{n+1} + \lambda_{n+1} L_{00}^{-1} \psi + c_{n+1} u_0,$$

where \widehat{w}_{n+1} is a real and localized particular solution to the w_{n+1} Eq. (5.15) but without the λ_{n+1} term on its right hand side, and c_{n+1} is a constant. This w_{n+1} solution is of the same form as w_n in (5.25) but with the index n changed to $n + 1$. This completes the induction process.

It is noted that in the above construction of the bifurcated eigenmodes, while λ_0 has two solutions $\lambda_{0\pm}$ (with $\lambda_{0+} = -\lambda_{0-}$) in view of Eq. (5.18), the higher coefficients $\lambda_1, \lambda_2, \dots$ as well as all (v_n, w_n) functions in the expansions (5.5)–(5.7) depend on λ_0^2 only and are thus the same for both values of $\lambda_{0\pm}$. It is then clear that the above construction yields two eigenmodes $(v_{\pm}^0, w_{\pm}^0, \lambda_{\pm}^0)$ which correspond to the two choices of the λ_0 values, and these two eigenmodes are related as

$$\lambda_+^0 = -\lambda_-^0, \quad v_+^0 = v_-^0, \quad w_+^0 = -w_-^0.$$

In addition, v_{\pm}^0 is always real, and $w_{\pm}^0, \lambda_{\pm}^0$ are either real or purely imaginary. The asymptotic formula for the eigenvalues λ_{\pm}^0 is

$$(\lambda^0)^2 \rightarrow -\lambda_0^2 (\mu - \mu_0), \quad \mu \rightarrow \mu_0, \tag{5.26}$$

where λ_0^2 is given in (5.18).

Finally, we simplify the λ_0^2 formula (5.18) and show that $-\lambda_0^2$ is equal to α as given in Eq. (3.8). To do so, we expand operator L_1 in (2.4) around $\mu = \mu_0$. Recalling the notations (2.5), we readily find L_{11} in the expansion (5.4) of L_1 as

$$L_{11} = G_2 u_1 - 1, \tag{5.27}$$

where u_1 is the $O(\mu - \mu_0)$ term in $u^0(\mathbf{x}; \mu)$'s expansion (5.3). The expression for u_1 has been obtained in Ref. [11] as

$$u_1 = L_{10}^{-1} u_0 + b_1 \psi, \tag{5.28}$$

where b_1 is a real constant. Inserting the above two expressions into (5.18) and recalling the condition $\langle G_2, \psi^3 \rangle = 0$ for pitchfork bifurcations in Theorem 1 as well as the definition of constant R in Eq. (2.7), we get a more explicit formula for λ_0^2 as

$$\lambda_0^2 = -\frac{R}{\langle \psi, L_{00}^{-1} \psi \rangle}. \tag{5.29}$$

In view of the conditions for pitchfork bifurcations in Theorem 1, we see that $\lambda_0^2 \neq 0$ as was mentioned before. Inserting this λ_0^2 formula into (5.26), the final asymptotic expression (3.7) for the bifurcated eigenvalues $\lambda^0(\mu)$ is then derived, with the constant α given by Eq. (3.8).

(b) Eigenvalue bifurcation along the bifurcated solution branches

Now we calculate eigenvalue bifurcations along the bifurcated solution branches $u^{\pm}(\mathbf{x}; \mu)$. For convenience, we assume that the bifurcation occurs for $\mu > \mu_0$ (when $RS > 0$, see Theorem 1). The other case of the bifurcation occurring for $\mu < \mu_0$ can be similarly

treated with trivial modifications, and both cases yield the same eigenvalue formula given in Eq. (3.9).

The bifurcated solitary waves near the bifurcation point $\mu = \mu_0$ have the following perturbation series expansion [11]

$$u^{\pm}(\mathbf{x}; \mu) = \sum_{k=0}^{\infty} (\mu - \mu_0)^{k/2} u_k(\mathbf{x}). \tag{5.30}$$

Since these solutions are assumed to exist on the right side of $\mu = \mu_0$, all functions u_1, u_2, \dots in this expansion are real-valued. Operators L_0 and L_1 on these bifurcated solution branches are expanded as

$$L_0^{\pm} = \sum_{k=0}^{\infty} (\mu - \mu_0)^{k/2} L_{0k}, \quad L_1^{\pm} = \sum_{k=0}^{\infty} (\mu - \mu_0)^{k/2} L_{1k}, \tag{5.31}$$

and all terms in these expansions are real-valued too. Note that quantities $u_k, L_{0k}, L_{1k}, k = 1, 2, \dots$ in these expansions are different from those in previous expansions (5.3)–(5.4). The linear-stability eigenmodes (v, w, λ) bifurcated from the zero eigenmode (3.2) now have the perturbation series expansions

$$v^{\pm}(\mathbf{x}; \mu) = \sum_{k=0}^{\infty} (\mu - \mu_0)^{k/2} v_k(\mathbf{x}), \tag{5.32}$$

$$w^{\pm}(\mathbf{x}; \mu) = \lambda_0 \sum_{k=0}^{\infty} (\mu - \mu_0)^{k/2} w_k(\mathbf{x}), \tag{5.33}$$

$$\lambda^{\pm}(\mu) = i\lambda_0 (\mu - \mu_0)^{1/2} \left(1 + \sum_{k=1}^{\infty} (\mu - \mu_0)^{k/2} \lambda_k \right). \tag{5.34}$$

Below we construct these perturbation series solutions to all orders.

Before this construction, we first derive a few relations on functions u_0, u_1, u_2 and u_3 in (5.30), which will be needed in later calculations. By inserting expansions (5.30) and (5.31) into Eqs. (2.16) and (2.17) and at suitable orders, we get the following relations

$$L_{01} u_0 = -L_{00} u_1, \tag{5.35}$$

$$L_{02} u_0 = -L_{01} u_1 - L_{00} u_2, \tag{5.36}$$

$$L_{11} u_1 = 2(u_0 - L_{10} u_2), \tag{5.37}$$

$$L_{12} u_1 = 2u_1 - 2L_{11} u_2 - 3L_{10} u_3. \tag{5.38}$$

In addition,

$$u_1 = b_1 \psi, \tag{5.39}$$

where $b_1 = \pm\sqrt{6R/S}$ which is non-zero [11]. Notice that b_1 is also real-valued here since $RS > 0$ by our earlier assumption.

We now substitute the perturbation expansions (5.32)–(5.34) into the linear-stability eigenvalue problem (2.15). From various orders of $(\mu - \mu_0)^{1/2}$, we get a sequence of linear equations for (v_k, w_k) as

$$L_{10} v_0 = 0, \tag{5.40}$$

$$L_{00} w_0 = 0, \tag{5.41}$$

$$L_{10} v_1 = \lambda_0^2 w_0 - L_{11} v_0, \tag{5.42}$$

$$L_{00} w_1 = v_0 - L_{01} w_0, \tag{5.43}$$

$$L_{10} v_2 = \lambda_0^2 (w_1 + \lambda_1 w_0) - (L_{11} v_1 + L_{12} v_0), \tag{5.44}$$

$$L_{00} w_2 = v_1 + \lambda_1 v_0 - (L_{01} w_1 + L_{02} w_0), \tag{5.45}$$

.....

$$L_{10} v_{n+1} = \lambda_0^2 \left(w_n + \sum_{k=1}^n \lambda_k w_{n-k} \right) - \sum_{k=1}^{n+1} L_{1k} v_{n+1-k}, \tag{5.46}$$

$$L_{00}w_{n+1} = v_n + \sum_{k=1}^n \lambda_k v_{n-k} - \sum_{k=1}^{n+1} L_{0k} w_{n+1-k}, \quad (5.47)$$

.....

In view of the assumption in Theorem 3, the solution to the v_0 Eq. (5.40), after eigenfunction rescaling, can be taken as

$$v_0 = u_1, \quad (5.48)$$

where u_1 is given in (5.39). The solution to the w_0 Eq. (5.41) is

$$w_0 = c_0 u_0, \quad (5.49)$$

where c_0 is a constant to be determined. When these (v_0, w_0) solutions are inserted into the (v_1, w_1) Eqs. (5.42)–(5.43) and relations (5.35), (5.37) utilized, we find that the solvability conditions of the (v_1, w_1) equations are automatically satisfied due to the condition of $\langle u_0, \psi \rangle = 0$ for pitchfork bifurcations in Theorem 1. These (v_1, w_1) equations admit localized solutions of the form

$$v_1 = 2(u_2 - L_{10}^{-1}u_0) + c_0 \lambda_0^2 L_{10}^{-1}u_0, \quad (5.50)$$

and

$$w_1 = L_{00}^{-1}u_1 + c_0 u_1 + c_1 u_0, \quad (5.51)$$

where $L_{10}^{-1}u_0$ and $L_{00}^{-1}u_1$ are localized real functions and c_1 is another constant. It is noted that the homogeneous solution (in proportion to u_1) to the v_1 equation is not included in the above v_1 solution since this term can be lumped into the v_0 term and then eliminated by a rescaling of the eigenfunction (v, w) —the same treatment we have applied previously in case (a) (see Eq. (5.19)).

Now we consider the (v_2, w_2) Eqs. (5.44)–(5.45). Inserting the above (v_0, v_1, w_0, w_1) solutions into the right hand side of the v_2 equation, utilizing the relations (5.35)–(5.38) and after simple algebra, the solvability condition of this v_2 equation, which requires that its right hand side be orthogonal to the homogeneous solution u_1 , yields

$$\lambda_0^2 = (2 - c_0 \lambda_0^2) \frac{\langle u_1, u_1 \rangle + 2\langle u_0, u_2 \rangle - 2\langle u_0, L_{10}^{-1}u_0 \rangle}{\langle u_1, L_{00}^{-1}u_1 \rangle}. \quad (5.52)$$

It is noted that u_1 is proportional to ψ and is nonzero, see Eq. (5.39). Thus due to the conditions (3.6), the denominator in the above equation is nonzero, i.e., $\langle u_1, L_{00}^{-1}u_1 \rangle \neq 0$. From the expansion (5.30) of the solutions $u^\pm(\mathbf{x}; \mu)$ and the condition $\langle u_0, \psi \rangle = 0$, we see that the expansion for the power function $P_\pm(\mu)$ is

$$P_\pm(\mu) = \langle u_0, u_0 \rangle + P'_\pm(\mu_0)(\mu - \mu_0) + O[(\mu - \mu_0)^{3/2}],$$

where

$$P'_\pm(\mu_0) = \langle u_1, u_1 \rangle + 2\langle u_0, u_2 \rangle \quad (5.53)$$

is the power slope at the bifurcation point $\mu = \mu_0$. From Eq. (2.10) in Theorem 2, we also know that

$$P'_+(\mu_0) = P'_-(\mu_0) = 2\langle u_0, L_{10}^{-1}u_0 \rangle + \frac{6R^2}{S}. \quad (5.54)$$

Using these relations as well as Eq. (5.39), the solvability condition (5.52) of the v_2 equation reduces to

$$\lambda_0^2 = (2 - c_0 \lambda_0^2) \frac{R}{\langle \psi, L_{00}^{-1}\psi \rangle}. \quad (5.55)$$

From the conditions for pitchfork bifurcations in Theorem 1, $R \neq 0$, thus $\lambda_0^2 \neq 0$.

Carrying similar calculations to the w_2 Eq. (5.45) and recalling the formula (2.9), the solvability condition of this w_2 equation yields

$$2 - c_0 \lambda_0^2 = \frac{2P'_\pm(\mu_0)}{P'_0(\mu_0)}. \quad (5.56)$$

When this equation is inserted into (5.55), an expression for λ_0^2 is then obtained as

$$\lambda_0^2 = \frac{2P'_\pm(\mu_0)}{P'_0(\mu_0)} \frac{R}{\langle \psi, L_{00}^{-1}\psi \rangle}, \quad (5.57)$$

which is real and nonzero. Inserting this λ_0^2 formula into (5.56), the constant c_0 can be obtained and is also real.

When λ_0 and c_0 are given by Eqs. (5.56)–(5.57), the solvability conditions of the (v_2, w_2) Eqs. (5.44)–(5.45) are satisfied. Utilizing the relation (5.35), the (v_2, w_2) solutions are of the form

$$v_2 = \widehat{v}_2 + \lambda_0^2(c_1 + \lambda_1 c_0)L_{10}^{-1}u_0,$$

and

$$w_2 = \widehat{w}_2 + \lambda_1 L_{00}^{-1}u_1 + c_1 u_1 + c_2 u_0,$$

where \widehat{v}_2 and \widehat{w}_2 are localized functions which satisfy Eqs. (5.44)–(5.45) but without the c_1 and λ_1 terms on their right hand sides, and c_2 is another constant. These constants λ_1, c_1 and c_2 will be determined from the solvability conditions of the higher (v_n, w_n) equations.

Using the method of induction and after straightforward algebra, we can show that the perturbation series solution (5.32)–(5.34) for the eigenmode (v, w, λ) can be determined to all orders. In addition, the (v_n, w_n) terms for $n \geq 2$ are of the form

$$v_n = \widehat{v}_n + \lambda_0^2(c_{n-1} + \lambda_{n-1}c_0)L_{10}^{-1}u_0, \quad n \geq 2,$$

and

$$w_n = \widehat{w}_n + \lambda_{n-1}L_{00}^{-1}u_1 + c_{n-1}u_1 + c_n u_0, \quad n \geq 2,$$

where \widehat{v}_n and \widehat{w}_n are certain localized functions, and $\lambda_{n-1}, c_{n-1}, c_n$ are constants. Since this induction calculation is analogous to that for case (a) in the earlier text, the details are omitted here.

In the above construction of the bifurcated eigenmodes, since λ_0 has two solutions from Eq. (5.57), two eigenmodes are then obtained. The eigenvalues of these two modes are either real or purely imaginary and are opposite of each other. From the perturbation expansion of these eigenvalues in Eq. (5.34) as well as Eq. (5.57), we see that the asymptotic formula for these eigenvalues near the bifurcation point is

$$(\lambda^\pm)^2 \rightarrow -\frac{2P'_\pm(\mu_0)}{P'_0(\mu_0)} \frac{R}{\langle \psi, L_{00}^{-1}\psi \rangle} (\mu - \mu_0), \quad \mu \rightarrow \mu_0,$$

which is the same as the formula (3.9) in Theorem 3. This completes the proof of Theorem 3. \square

Proof of Theorem 4. From the assumptions in Theorem 4, the solitary wave $u_0(\mathbf{x})$ at the bifurcation point $\mu = \mu_0$ is linearly stable; and when $0 < |\mu - \mu_0| \ll 1$, the only instability-inducing eigenvalue bifurcation is from the origin. In Theorem 3, we have shown that from the origin, a single pair of eigenvalues $\pm\lambda$ in \mathcal{L} bifurcate out along the real or imaginary axis. Thus the linear stability of these solitary waves near $\mu = \mu_0$ is determined entirely by whether this pair of eigenvalues are real or purely imaginary. On the base solitary wave branch $u^0(\mathbf{x}; \mu)$, this pair of eigenvalues are given asymptotically by Eq. (3.7). Thus if $\alpha > 0$, these eigenvalues are real when $\mu > \mu_0$ and imaginary when $\mu < \mu_0$, hence the solitary waves are linearly unstable when $\mu > \mu_0$ and linearly stable when $\mu < \mu_0$. If $\alpha < 0$, the situation is just the opposite. In both cases, stability switches at the bifurcation point. On the bifurcated solitary branches $u^\pm(\mathbf{x}; \mu)$, the bifurcated eigenvalues are given asymptotically by Eq. (3.9). The formula (3.10) for the constant β shows that when the two power slopes $P'_0(\mu_0)$ and $P'_\pm(\mu_0)$ have the same sign, β and α would have the opposite sign, meaning that eigenvalues for the $u^\pm(\mathbf{x}; \mu)$ and $u^0(\mathbf{x}; \mu)$ branches bifurcate along perpendicular directions from the origin, hence these solu-

tion branches have opposite linear stability. On the other hand, if the two power slopes $P'_0(\mu_0)$ and $P'_\pm(\mu_0)$ have the opposite sign, β and α would have the same sign, hence the $u^\pm(\mathbf{x}; \mu)$ and $u^0(\mathbf{x}; \mu)$ branches would have the same linear stability. This completes the proof of Theorem 4. \square

Proof of Theorem 5. First of all, due to Remark 4, L_{10} has one or more positive discrete eigenvalues. If L_{10} has more than one positive discrete eigenvalue, then the positive solitary wave $u_0(\mathbf{x})$ at the bifurcation point $\mu = \mu_0$ is linearly unstable by the generalized Vakhitov–Kolokolov stability criterion (see [13, Theorem 5.2, p. 176]). If L_{10} has only one positive discrete eigenvalue and $P'_0(\mu_0) < 0$, since $\langle u_0, \psi \rangle = 0$ by the conditions of pitchfork bifurcations in Theorem 1, the positive solitary wave $u_0(\mathbf{x})$ is then linearly unstable by the generalized Vakhitov–Kolokolov stability criterion (see [13, Theorem 5.2]). When $u_0(\mathbf{x})$ is linearly unstable, solitary waves near the bifurcation point $\mu = \mu_0$ are clearly also linearly unstable.

Next we consider the case when L_{10} has only one positive discrete eigenvalue, $P'_0(\mu_0) > 0$, and $P'_\pm(\mu_0) \neq 0$. In this case, since $\langle u_0, \psi \rangle = 0$, $u_0(\mathbf{x})$ at the bifurcation point is linearly stable by the generalized Vakhitov–Kolokolov stability criterion (Ref. [13, Theorem 5.2]). In addition, since the solitary waves near the bifurcation point are positive, all eigenvalues in \mathcal{L} are real or purely imaginary (Ref. [13, Theorem 5.2]), thus no complex eigenvalues can bifurcate out when $\mu \neq \mu_0$. So the assumptions in Theorem 4 are satisfied. Since $u_0(\mathbf{x})$ is positive, zero is then the largest eigenvalue of L_{00} and is simple [27], and $\langle \psi, L_{00}^{-1}\psi \rangle < 0$ as L_{00} is semi-negative definite and $\psi \neq 0$. In addition, zero is a simple eigenvalue of L_{10} , $P'_0(\mu_0) \neq 0$ and $P'_\pm(\mu_0) \neq 0$ by our assumptions above. Thus the conditions of Theorem 4 are also met. Hence Theorem 4 can be applied. Using this theorem, together with Remark 3 and the fact of $\langle \psi, L_{00}^{-1}\psi \rangle < 0$, we can then prove the results in the four cases of Theorem 5 as below.

- (1) When the bifurcation occurs for $\mu > \mu_0$ and $P'_\pm(\mu_0) < P'_0(\mu_0)$, α is positive by Remark 3. Then by Theorem 4, the base solution branch $u^0(\mathbf{x}; \mu)$ is stable for $\mu < \mu_0$ and unstable for $\mu > \mu_0$. Regarding the bifurcated branches, they and the unstable base branch (on the right side of $\mu = \mu_0$) have the opposite (same) stability when $P'_0(\mu_0)$ and $P'_\pm(\mu_0)$ have the same (opposite) sign. Since $P'_0(\mu_0) > 0$, these bifurcated branches are then stable when $P'_\pm(\mu_0) > 0$ and unstable when $P'_\pm(\mu_0) < 0$.
- (2) When the bifurcation occurs for $\mu > \mu_0$ and $P'_\pm(\mu_0) > P'_0(\mu_0) > 0$, α is negative by Remark 3. Thus the base solution branch is unstable for $\mu < \mu_0$ and stable for $\mu > \mu_0$. Since $P'_\pm(\mu_0)$ and $P'_0(\mu_0)$ are now both positive, the bifurcated branches then have the opposite stability of the stable base branch (on the right side of $\mu = \mu_0$) and are thus always unstable.
- (3) When the bifurcation occurs for $\mu < \mu_0$ and $P'_\pm(\mu_0) < P'_0(\mu_0)$, α is negative by Remark 3. Then by Theorem 4, the base solution branch is unstable for $\mu < \mu_0$ and stable for $\mu > \mu_0$. The bifurcated branches (with $\mu < \mu_0$) are stable (opposite of the unstable base branch) if $P'_\pm(\mu_0) > 0$ and unstable (same as the unstable base branch) if $P'_\pm(\mu_0) < 0$.
- (4) When the bifurcation occurs for $\mu < \mu_0$ and $P'_\pm(\mu_0) > P'_0(\mu_0) > 0$, α is positive by Remark 3; hence by Theorem 4, the base solution branch is stable for $\mu < \mu_0$ and unstable for $\mu > \mu_0$. Since both $P'_\pm(\mu_0)$ and $P'_0(\mu_0)$ are now positive, the bifurcated branches are always unstable (opposite of the stable base branch on the left side of $\mu = \mu_0$). This completes the proof of Theorem 5. \square

Proof of Lemma 1. First we study eigenvalue bifurcation in operator L_1^0 along the base branch $u^0(\mathbf{x}; \mu)$. This eigenvalue problem is

$$L_1^0 \Psi = \Lambda_0 \Psi, \tag{5.58}$$

where $\Lambda_0(\mu)$ is the eigenvalue of L_1^0 . When $\mu = \mu_0$, $\Lambda_0(\mu_0) = 0$, and $\Psi(\mathbf{x}; \mu_0) = \psi$. To determine $\Lambda_0(\mu)$ for $|\mu - \mu_0| \ll 1$, we use the perturbation method. The perturbation expansion for operator L_1^0 has been given in Eq. (5.4). Perturbation expansions for Ψ and Λ_0 are

$$\begin{aligned} \Psi(\mathbf{x}; \mu) &= \psi + (\mu - \mu_0)\Psi_1 + (\mu - \mu_0)^2\Psi_2 + \dots, \\ \Lambda_0(\mu) &= c_1(\mu - \mu_0) + c_2(\mu - \mu_0)^2 + \dots. \end{aligned}$$

Substituting these expansions into (5.58), the $O(1)$ equation is automatically satisfied. At $O(\mu - \mu_0)$, we get

$$L_{10}\Psi_1 = c_1\psi - L_{11}\psi.$$

The Fredholm solvability condition of this equation is that its right hand side be orthogonal to the homogeneous solution ψ . This condition yields

$$c_1 = \frac{\langle \psi, L_{11}\psi \rangle}{\langle \psi, \psi \rangle}.$$

Utilizing Eqs. (5.27) and (5.28), we can simplify c_1 as

$$c_1 = -\frac{R}{\langle \psi, \psi \rangle}.$$

Hence formula (4.7) in Lemma 1 is proved.

Next we study eigenvalue bifurcation in operator L_1^\pm along the bifurcated branches $u^\pm(\mathbf{x}; \mu)$. This eigenvalue problem is

$$L_1^\pm \Psi = \Lambda_\pm \Psi, \tag{5.59}$$

where $\Lambda_\pm(\mu)$ is the eigenvalue of L_1^\pm , and $\Lambda_\pm(\mu_0) = 0$. When $|\mu - \mu_0| \ll 1$, the perturbation expansion for operator L_1^\pm has been given in Eq. (5.31). Perturbation expansions for Ψ and Λ_\pm are

$$\begin{aligned} \Psi(\mathbf{x}; \mu) &= \Psi_0 + (\mu - \mu_0)^{1/2}\Psi_1 + (\mu - \mu_0)\Psi_2 + \dots, \\ \Lambda_\pm(\mu) &= d_1(\mu - \mu_0)^{1/2} + d_2(\mu - \mu_0) + \dots. \end{aligned}$$

Substituting these expansions into (5.59), the $O(1)$ equation is

$$L_{10}\Psi_0 = 0.$$

For convenience, we take the Ψ_0 solution as

$$\Psi_0 = u_1, \tag{5.60}$$

where u_1 is the second term in the perturbation expansion (5.30) of the bifurcated solutions $u^\pm(\mathbf{x}; \mu)$, and its expression is given in Eq. (5.39).

At $O((\mu - \mu_0)^{1/2})$, Eq. (5.59) gives

$$L_{10}\Psi_1 = d_1u_1 - L_{11}u_1, \tag{5.61}$$

whose solvability condition yields

$$d_1 = \frac{\langle u_1, L_{11}u_1 \rangle}{\langle u_1, u_1 \rangle}.$$

Inserting Eqs. (5.37) and (5.39) into the above expression and recalling that L_{10} is self-adjoint and has ψ in its kernel, we readily see that

$$d_1 = 0.$$

Then substituting (5.37) into (5.61), we get

$$\Psi_1 = 2u_2 - 2L_{10}^{-1}u_0. \tag{5.62}$$

At $O(\mu - \mu_0)$, Eq. (5.59) gives

$$L_{10}\Psi_2 = d_2u_1 - L_{12}u_1 - L_{11}\Psi_1 \tag{5.63}$$

whose solvability condition yields

$$d_2 = \frac{\langle u_1, L_{12}u_1 \rangle + \langle L_{11}u_1, \Psi_1 \rangle}{\langle u_1, u_1 \rangle}.$$

Inserting Eqs. (5.37), (5.38) and (5.62) into the above equation and after simple algebra, we get

$$d_2 = 2 \frac{\langle u_1, u_1 \rangle + 2\langle u_0, u_2 \rangle - 2\langle u_0, L_{10}^{-1}u_0 \rangle}{\langle u_1, u_1 \rangle}.$$

Finally, utilizing Eqs. (5.39), (5.53) and (5.54), we get

$$d_2 = \frac{2R}{\langle \psi, \psi \rangle},$$

thus formula (4.8) in Lemma 1 is proved. \square

6. Numerical examples

In this section, we use a few numerical examples to illustrate and confirm the above analytical stability results. These examples contain both positive and sign-indefinite solitary waves in double-well and periodic potentials under focusing and defocusing nonlinearities in one and higher spatial dimensions.

Example 1. Our first example is the one-dimensional GNLS equation (2.1) with a symmetric double-well potential and cubic-quintic nonlinearity,

$$iU_t + U_{xx} - V(x)U + |U|^2U - 0.25|U|^4U = 0, \tag{6.1}$$

where the symmetric double-well potential $V(x)$ is taken as

$$V(x) = -2.8 [\operatorname{sech}^2(x + 1.5) + \operatorname{sech}^2(x - 1.5)] \tag{6.2}$$

and is shown in Fig. 4(a). Pitchfork bifurcations of positive solitary waves in this equation have been reported in [11], and the power diagram for these bifurcations is displayed in Fig. 4(b). This power diagram shows that two pitchfork bifurcations occur at points ‘A, B’ of the power diagram. At positions ‘c, d, e’, profiles of solitary waves are shown in Fig. 4(c), (d) and (e) respectively. It is seen that solitary waves at positions ‘c, d’ are symmetric, while solitary waves at position ‘e’ are asymmetric. Thus symmetry-breaking bifurcations occur at both ‘A, B’ points. In particular, the c–d power branch is the symmetric (base) branch, and the e-branch is the asymmetric (bifurcated) branch.

Since solitary waves in this example are positive, Theorem 5 applies. It is known that for both pitchfork bifurcations at points ‘A, B’, L_{10} has a single positive discrete eigenvalue [11]. In addition, the power diagram in Fig. 4(b) shows that at both ‘A, B’ points, $0 < P'_\pm(\mu_0) < P'_0(\mu_0)$. Thus Theorem 5 (case 1) predicts that near the bifurcation point ‘A’, the stability information would be as shown in Fig. 2(b). Theorem 5 (case 3) also predicts that near the bifurcation point ‘B’, the stability information would be as shown in Fig. 3(b).

Numerically we have found that these analytical predictions are entirely correct. Specifically, we have found numerically that the segment of the symmetric branch between points ‘A, B’ is linearly unstable, and the other segments/branches of the power diagram are all linearly stable. This stability information is indicated by the solid blue and dashed red lines in Fig. 4(b) for stable and unstable solutions respectively. We can see that near the bifurcation points ‘A, B’, these power-stability diagrams agree with Figs. 2(b) and 3(b) predicted by Theorem 5. To corroborate these stability results, the linear-stability spectra for solitary waves at locations ‘c, d, e’ of the power diagram are numerically computed by the Fourier collocation method [13], and the results are displayed in Fig. 4(f), (g) and (h). It is seen that the spectrum at ‘d’ contains a positive eigenvalue, hence its symmetric solitary wave is linearly unstable. The spectra at ‘c, e’, on the other hand, lie entirely on the imaginary axis, thus those solitary waves are linearly stable.

These numerical stability results agree completely with the above analytical predictions.

The reader may notice that the asymmetric ‘e’-branch in Fig. 4(b) contains two additional saddle–node (fold) bifurcations. As was explained in [20,21], there is no stability switching at saddle–node bifurcations in the GNLS equations (2.1), thus it is not surprising that the entire asymmetric ‘e’-branch in Fig. 4(b) is linearly stable despite these saddle–node bifurcations.

Example 2. Our second example is the one-dimensional GNLS equation (2.1) with self-focusing cubic nonlinearity and a periodic potential,

$$iU_t + U_{xx} - V(x)U + |U|^2U = 0, \tag{6.3}$$

where the periodic potential $V(x)$ is

$$V(x) = 6 \sin^2 x. \tag{6.4}$$

This equation admits infinite families of multi-hump solitary waves (2.2) which all exhibit pitchfork bifurcations [10]. The power curve for one such family of sign-indefinite solitary waves in the semi-infinite bandgap is shown in Fig. 5(a). The first Bloch band of this periodic potential is $\mu \in [-2.2667, -2.0632]$, which is located to the left side of this power diagram. This power diagram contains three branches which are connected with each other. At the intersection point ‘A’ between the lower and middle branches, a pitchfork bifurcation occurs. This pitchfork bifurcation is better seen in Fig. 5(b), which shows an amplification of the power diagram in Fig. 5(a) around this intersection point. Solitary waves on the lower power branch are anti-symmetric (see Fig. 5(c)), whereas solitary waves on the middle power branch are asymmetric (see Fig. 5(d)), hence a symmetry-breaking bifurcation occurs at point ‘A’.

At this bifurcation point ‘A’, we have checked numerically that $\langle \psi, L_{00}^{-1}\psi \rangle < 0$. We have also checked that the solitary wave at point ‘A’ is linearly stable, and near this bifurcation point no complex eigenvalues appear. Thus the power diagram in Fig. 5(b) predicts that the stability information near this bifurcation point would be as given in Fig. 2(a).

Numerically we have found that these analytical predictions are again all correct. Specifically, we have determined the stability of these solitary waves through computation of their linear-stability spectra, and the stability results are indicated on the power diagram in Fig. 5(a) and (b), where the stable and unstable branches are marked as solid blue and dashed red lines respectively. We see that these stability results are in full agreement with the analytical predictions in Fig. 2(a). To corroborate these stability results, the full linear-stability spectra for solitary waves at locations ‘c, d’ of Fig. 5(a) are displayed in Fig. 5(e) and (f). These spectra confirm that the anti-symmetric solitary wave (Fig. 5(c)) at location ‘c’ of the lower power branch is indeed linearly stable, whereas the asymmetric solitary wave (Fig. 5(d)) at location ‘d’ of the middle branch is indeed linearly unstable. The unstable eigenvalue at location ‘d’ is real positive, and it bifurcates out from the pitchfork bifurcation point ‘A’, in agreement with our theory.

Example 3. Our third example is the seventh-power GNLS equation with a symmetric double-well potential,

$$iU_t + U_{xx} - V(x)U + |U|^6U = 0, \tag{6.5}$$

where the double-well potential $V(x)$ is

$$V(x) = -3 \operatorname{sech}^2(x + 1) - 3 \operatorname{sech}^2(x - 1), \tag{6.6}$$

which is shown in Fig. 6(b). This equation admits a family of positive solitary waves whose power diagram is displayed in

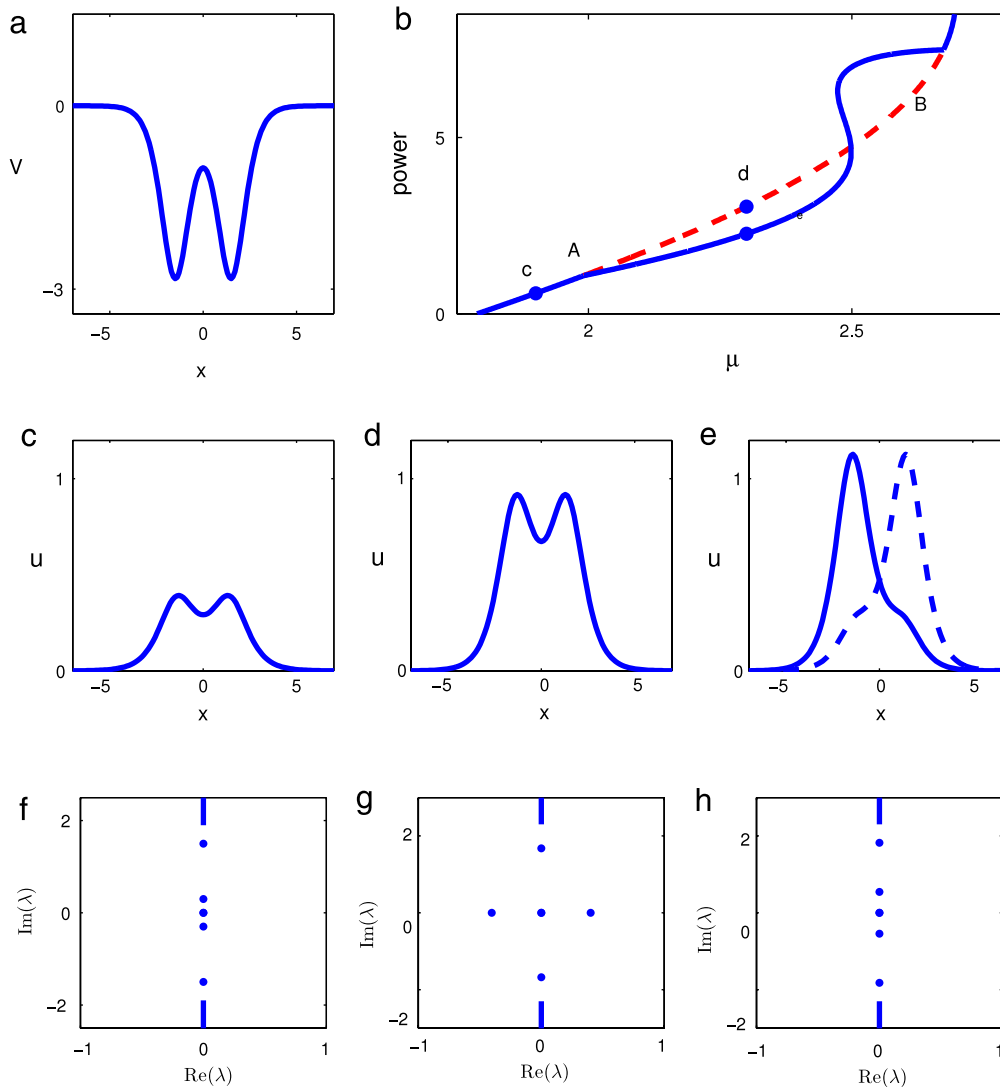


Fig. 4. (Color online) Pitchfork bifurcations of solitary waves and their linear-stability behaviors in Example 1. (a) The potential (6.2); (b) the power-stability diagram (solid blue and dashed red indicate stable and unstable solutions respectively); (c), (d) and (e) profiles of solitary waves at positions of the same letters in (b); the two asymmetric solitary waves in (e) are mirror images of each other with respect to x ; (f), (g) and (h) linear-stability spectra of the solitary waves in (c), (d) and (e) respectively.

Fig. 6(a). This power diagram shows that a pitchfork bifurcation occurs at the point 'A'. On the upper b - c_1 branch, solitary waves are symmetric (see Fig. 6(b) and (c)), whereas on the lower c_2 branch, solitary waves are asymmetric (see Fig. 6(c)).

At the pitchfork bifurcation point 'A', we have checked that L_{10} has a single positive discrete eigenvalue. Thus from the power diagram in Fig. 6(a), Theorem 5 (case 1) predicts that the stability information near this bifurcation point is as given in Fig. 2(c). This analytical prediction fully agrees with the numerical stability results in Fig. 6(a) (where the stable and unstable solutions are indicated). These stability results are further corroborated in Fig. 6(d), (e) and (f), where linear-stability spectra for solitary waves at locations 'b, c_1 , c_2 ' are displayed.

In this example, after the pitchfork bifurcation occurs (i.e., on the right side of 'A'), both the symmetric and asymmetric solution branches are linearly unstable. A similar bifurcation was reported numerically in [8] for the eleventh-power nonlinearity but was not found for the present seventh-power nonlinearity. This seventh power nonlinearity is below the nonlinearity threshold $4 + \sqrt{13} \approx 7.6056$ for this type of pitchfork bifurcation in the semi-classical limit (i.e., large well-separation limit) [6,8]. This bifurcation can still occur for the seventh-power nonlinearity in Eq. (6.5) because the separation between the two potential wells in (6.6) is not large.

Example 4. Our last example is the two-dimensional GNLs equation with self-defocusing cubic nonlinearity and a symmetric double-well potential,

$$iU_t + U_{xx} + U_{yy} - V(x, y)U - |U|^2U = 0, \quad (6.7)$$

where the double-well potential $V(x, y)$ is

$$V(x, y) = -6 \left(e^{-[(x+1.5)^2+y^2]} + e^{-[(x-1.5)^2+y^2]} \right), \quad (6.8)$$

which is shown in Fig. 7(a). This equation admits a family of sign-indefinite solitary waves (2.2) whose power diagram is given in Fig. 7(b). It is seen that a pitchfork bifurcation occurs at the point 'A'. At positions 'd, e, f' of the power diagram, profiles of the solitary waves are displayed in Fig. 7(d), (e) and (f). Solitary waves at 'd, e' are anti-symmetric in x and symmetric in y , whereas the solitary wave at 'f' is asymmetric in x and symmetric in y . Thus this pitchfork bifurcation is also a symmetry-breaking bifurcation.

At this bifurcation point, we have checked numerically that $\langle \psi, L_{00}^{-1} \psi \rangle > 0$. In addition, the solitary wave at point 'A' is linearly stable, and the solitary waves nearby do not possess complex eigenvalues. Thus the power diagram in Fig. 7(b) predicts that the stability information is as given in Fig. 3(e) but with the stability of

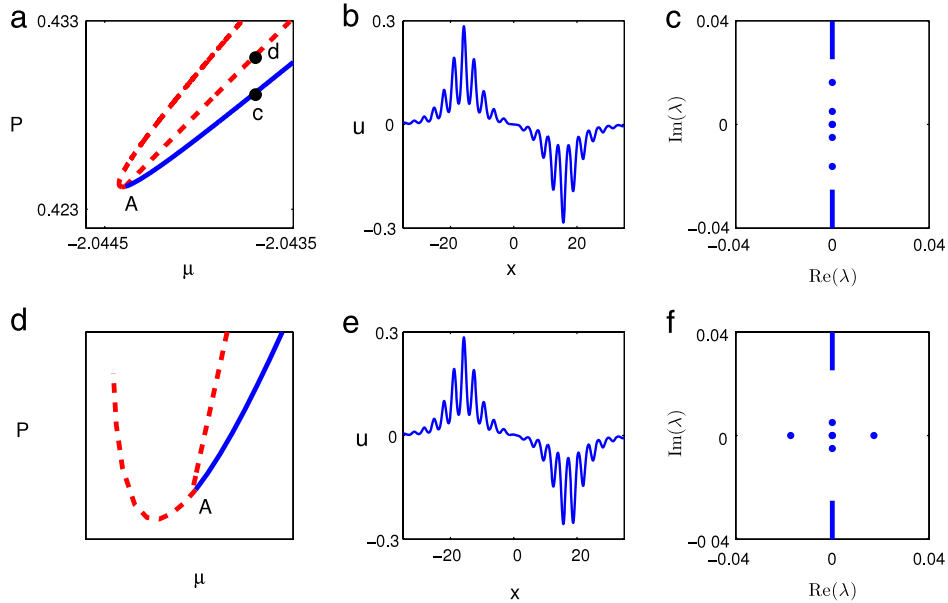


Fig. 5. (Color online) Pitchfork bifurcations of solitary waves and their linear-stability behaviors in Example 2. (a) The power-stability diagram (solid blue for stable solutions and dashed red for unstable ones); (b) amplification of the power-stability diagram in (a) near the pitchfork bifurcation point ‘A’; (c), (d) profiles of solitary waves at locations ‘c’, ‘d’ of the power diagram in (a); (e), (f) linear-stability spectra for solitary waves in (c), (d) respectively.

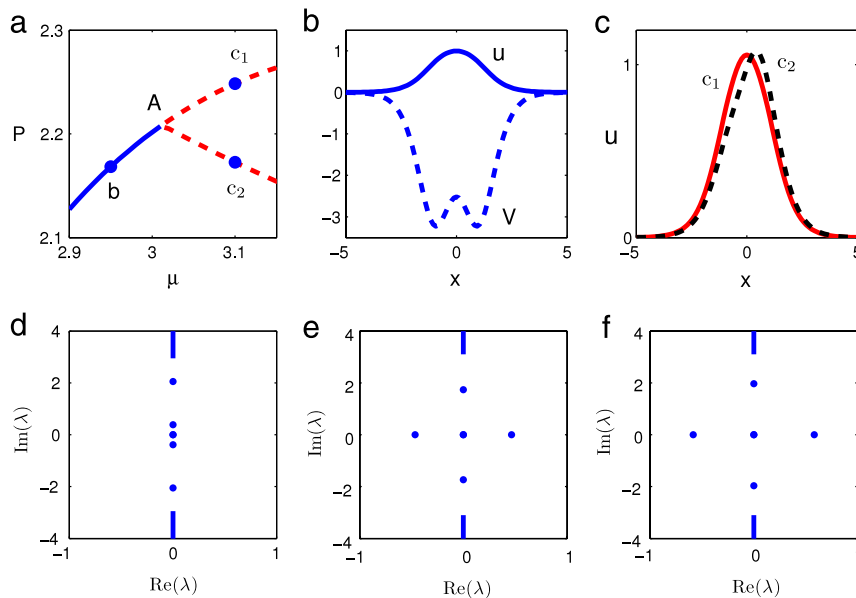


Fig. 6. (Color online) Pitchfork bifurcations of solitary waves and their linear-stability behaviors in Example 3. (a) The power-stability diagram (solid blue is stable and dashed red unstable); (b) profiles of the potential $V(x)$ (dashed) and the solitary wave (solid) at location ‘b’ of the power diagram; (c) solitary wave profiles at locations ‘ c_1 ’ (solid) and ‘ c_2 ’ (dashed) of the power diagram; (e), (f) and (g) linear-stability spectra for solitary waves at locations ‘b’, c_1 , c_2 ’ respectively.

each branch flipped (because $\langle \psi, L_{00}^{-1} \psi \rangle > 0$ here). This prediction agrees with our numerical stability results shown in Fig. 7(b). The numerical-stability results are further illustrated in Fig. 7(g), (h) and (i), where the stability spectra for solitary waves in Fig. 7(d), (e) and (f) are displayed. These spectra corroborate the numerical-stability results in the power diagram of Fig. 7(b) and support our analytical predictions.

In the previous examples, our comparison between analytical and numerical stability results was qualitative. Here for this Example 4, we will also make a quantitative comparison on unstable eigenvalues in order to completely verify our eigenvalue formulae in Theorem 3. Specifically, we notice that the anti-symmetric solution branch in Fig. 7(b) is unstable on the left side of ‘A’, and this instability is induced by a positive eigenvalue which is predicted analytically by the formula (3.7) in Theorem 3.

Numerically we have determined this unstable eigenvalue λ^0 for various values of μ by the highly-accurate Newton-conjugate-gradient method [13], and these numerical eigenvalues are plotted in Fig. 7(c) as blue squares. Further examination of this numerical data shows that as $\mu \rightarrow \mu_0$, where $\mu_0 \approx 1.9072149$ is the propagation-constant value at the bifurcation point ‘A’, the numerical eigenvalue λ^0 behaves as

$$(\lambda^0)_{num}^2 \rightarrow \alpha_{num}(\mu - \mu_0), \quad \mu \rightarrow \mu_0, \tag{6.9}$$

where the numerical coefficient is

$$\alpha_{num} \approx -0.3788744.$$

In the analytical eigenvalue formula (3.7), the coefficient α from formula (3.8) is found to be

$$\alpha_{anal} \approx -0.3788744.$$

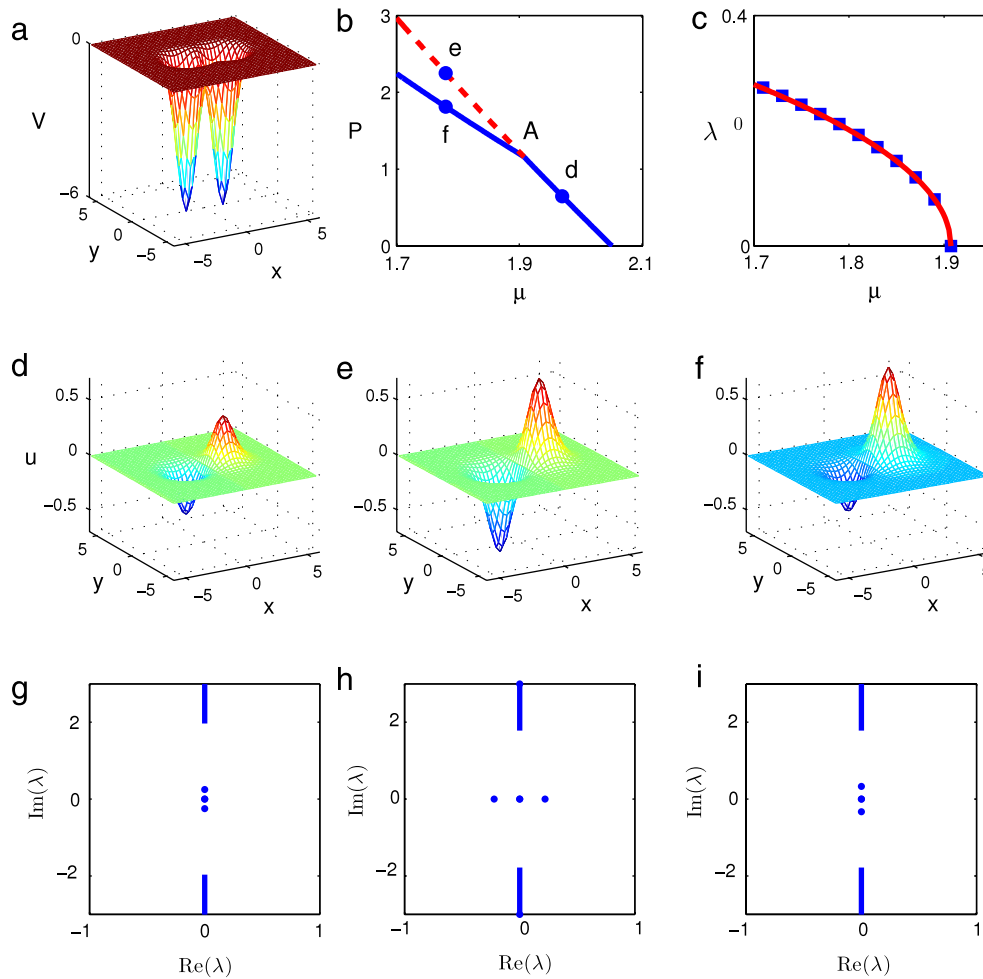


Fig. 7. (Color online) Pitchfork bifurcations of solitary waves and their linear-stability behaviors in Example 4. (a) The two-dimensional double-well potential (6.8); (b) the power-stability diagram (solid blue is stable and dashed red unstable); (c) the unstable eigenvalue λ^0 versus μ on the anti-symmetric solution branch of (b) (blue squares: numerical values; red solid line: analytical prediction from formula (3.7)); (d), (e) and (f) profiles of solitary waves at locations 'd, e, f' of the power diagram in (b); (g), (h) and (i) stability spectra for solitary waves in (d), (e) and (f) respectively.

We see that the numerical eigenvalue formula (6.9) and the analytical formula (3.7) are in complete quantitative agreement.

On the bifurcated asymmetric solution branch in Fig. 7(b), the solitary waves possess a pair of purely imaginary discrete eigenvalues which are predicted analytically by the formula (3.9) in Theorem 3. We have quantitatively compared the numerical values of those imaginary eigenvalues against the analytical formula (3.9) and found complete agreement as well. Thus both eigenvalue formulae (3.7) and (3.9) in Theorem 3 are numerically verified.

7. Summary and discussion

In this article, linear stability of both sign-definite (positive) and sign-indefinite solitary waves near pitchfork bifurcations has been analyzed for the generalized nonlinear Schrödinger equations (2.1) with arbitrary forms of nonlinearity and external potentials in arbitrary spatial dimensions. Bifurcations of linear-stability eigenvalues associated with these pitchfork bifurcations have been analytically calculated, and their expressions are given by the formulae (3.7) and (3.9) in Theorem 3. An important feature of these eigenvalue formulae is that they are intimately related to the power slopes of solution branches at the bifurcation point. Based on these eigenvalue formulae, linear stability of solitary waves near pitchfork bifurcations is then determined (see Theorem 4).

In this article, we have shown that for pitchfork bifurcations in the GNLS equations (2.1), the base solution branch $u^0(\mathbf{x}; \mu)$

always switches stability at the bifurcation point. In addition, the bifurcated solution branches $u^\pm(\mathbf{x}; \mu)$ and the base branch have opposite (same) stability when their power slopes $P'_0(\mu_0)$ and $P'_\pm(\mu_0)$ have the same (opposite) sign. Furthermore, if the sign of $\langle \psi, L_{00}^{-1} \psi \rangle$ is known, then the stability of solitary waves near the bifurcation point can be read off directly from the power diagram (see Figs. 2 and 3). This determination of stability from the power diagram applies particularly to positive solitary waves, where $\langle \psi, L_{00}^{-1} \psi \rangle$ is known to be always negative (see Theorem 5). These stability results are also compared with the Hamiltonian–Krein index theory (see Section 4), and it is shown that the qualitative stability results can also be derived by the index theory (under more restrictive conditions). Lastly, a number of numerical examples of pitchfork bifurcations in Eq. (2.1) have been presented. These examples include double-well or periodic potentials, and focusing or defocusing nonlinearities of Kerr (cubic) or non-Kerr types. The numerical results fully support the analytical predictions both qualitatively and quantitatively.

One unusual feature of these pitchfork bifurcations in the GNLS equations is that the base and bifurcated solution branches (on the same side of the bifurcation point) can be both stable or both unstable, which contrasts such bifurcations in finite-dimensional dynamical systems where the base and bifurcated branches generally have opposite stability [18].

It is noted that the linear-stability analysis for pitchfork bifurcations in this article is related to normal forms for these

bifurcations [9,34], just like linear stability of fixed points is related to normal forms in finite-dimensional dynamical systems [18]. Thus one can rederive the linear-stability results in this article by normal-form calculations.

Acknowledgments

The author is indebted to Dr. Todd Kapitula for showing him how to apply the Hamiltonian–Krein index theory to this bifurcation problem (see Section 4). He also thanks the anonymous referees for many helpful suggestions which improved the clarity of the manuscript. This work is supported in part by the Air Force Office of Scientific Research (USAF 9550-09-1-0228) and the National Science Foundation (DMS-0908167).

References

- [1] R.K. Jackson, M.I. Weinstein, Geometric analysis of bifurcation and symmetry breaking in a Gross–Pitaevskii equation, *J. Stat. Phys.* 116 (2004) 881–905.
- [2] P.G. Kevrekidis, Z. Chen, B.A. Malomed, D.J. Frantzeskakis, M.I. Weinstein, Spontaneous symmetry breaking in photonic lattices: theory and experiment, *Phys. Lett. A* 340 (2005) 275–280.
- [3] M. Matuszewski, B.A. Malomed, M. Trippenbach, Spontaneous symmetry breaking of solitons trapped in a double-channel potential, *Phys. Rev. A* 75 (2007) 063621.
- [4] E.W. Kirr, P.G. Kevrekidis, E. Shlizerman, M.I. Weinstein, Symmetry-breaking bifurcation in nonlinear Schrödinger/Gross–Pitaevskii equations, *SIAM J. Math. Anal.* 40 (2008) 56–604.
- [5] M. Trippenbach, E. Infeld, J. Gocialek, M. Matuszewski, M. Oberthaler, B.A. Malomed, Spontaneous symmetry breaking of gap solitons and phase transitions in double-well traps, *Phys. Rev. A* 78 (2008) 013603.
- [6] A. Sacchetti, Universal critical power for nonlinear Schrödinger equations with symmetric double well potential, *Phys. Rev. Lett.* 103 (2009) 194101.
- [7] C. Wang, G. Theocharis, P.G. Kevrekidis, N. Whitaker, K.J.H. Law, D.J. Frantzeskakis, B.A. Malomed, Two-dimensional paradigm for symmetry breaking: the nonlinear Schrödinger equation with a four-well potential, *Phys. Rev. E* 80 (2009) 046611.
- [8] E.W. Kirr, P.G. Kevrekidis, D.E. Pelinovsky, Symmetry-breaking bifurcation in the nonlinear Schrödinger equation with symmetric potentials, *Comm. Math. Phys.* 308 (2011) 795–844.
- [9] D.E. Pelinovsky, T. Phan, Normal form for the symmetry-breaking bifurcation in the nonlinear Schrödinger equation, *J. Differential Equations* 253 (2012) 2796–2824.
- [10] T.R. Akylas, G. Hwang, J. Yang, From nonlocal gap solitary waves to bound states in periodic media, *Proc. Roy. Soc. A* 468 (2012) 116–135.
- [11] J. Yang, Classification of solitary wave bifurcations in generalized nonlinear Schrödinger equations, *Stud. Appl. Math.* 129 (2012) 133–162.
- [12] Y.S. Kivshar, G.P. Agrawal, *Optical Solitons: From Fibers to Photonic Crystals*, Academic Press, San Diego, 2003.
- [13] J. Yang, *Nonlinear Waves in Integrable and Nonintegrable Systems*, SIAM, Philadelphia, 2010.
- [14] L.P. Pitaevskii, S. Stringari, *Bose–Einstein Condensation*, Oxford University Press, Oxford, 2003.
- [15] N. Akhmediev, A. Ankiewicz, Novel soliton states and bifurcation phenomena in nonlinear fiber couplers, *Phys. Rev. Lett.* 70 (1993) 2395–2398.
- [16] H. Sakaguchi, B.A. Malomed, Symmetry breaking of solitons in two-component Gross–Pitaevskii equations, *Phys. Rev. E* 83 (2011) 036608.
- [17] Y.V. Kartashov, B.A. Malomed, L. Torner, Solitons in nonlinear lattices, *Rev. Mod. Phys.* 83 (2011) 247–306.
- [18] J. Guckenheimer, P. Holmes, *Nonlinear Oscillations, Dynamical Systems, and Bifurcations of Vector Fields*, Springer-Verlag, New York, 1990.
- [19] G. Hwang, T.R. Akylas, J. Yang, Solitary waves and their linear stability in nonlinear lattices, *Stud. Appl. Math.* 128 (2012) 275–299.
- [20] J. Yang, No stability switching at saddle–node bifurcations of solitary waves in generalized nonlinear Schrödinger equations, *Phys. Rev. E* 85 (2012) 037602.
- [21] J. Yang, Conditions and stability analysis for saddle–node bifurcations of solitary waves in generalized nonlinear Schrödinger equations, in: B.A. Malomed (Ed.), *Spontaneous Symmetry Breaking, Self-Trapping, and Josephson Oscillations in Nonlinear Systems*, Springer, Berlin, 2012 (Chapter in book).
- [22] Y. Pomeau, A. Ramani, B. Grammaticos, Structural stability of the Kortewegde Vries solitons under a singular perturbation, *Physica D* 31 (1988) 127–134.
- [23] R. Grimshaw, Weakly nonlocal solitary waves in a singularly perturbed nonlinear Schrödinger equation, *Stud. Appl. Math.* 94 (1995) 257–270.
- [24] D.C. Calvo, T.R. Akylas, On the formation of bound states by interacting nonlocal solitary waves, *Physica D* 101 (1997) 270–288.
- [25] D.E. Pelinovsky, A.A. Sukhorukov, Y.S. Kivshar, Bifurcations and stability of gap solitons in periodic potentials, *Phys. Rev. E* 70 (2004) 036618.
- [26] G. Hwang, T.R. Akylas, J. Yang, Gap solitons and their linear stability in one-dimensional periodic media, *Physica D* 240 (2011) 1055–1068.
- [27] M. Struwe, *Variational Methods: Applications to Nonlinear Partial Differential Equations and Hamiltonian Systems*, third ed., Springer, Berlin, 2000 (Specifically the paragraph just below Theorem B.4 on p. 246).
- [28] T. Kapitula, P. Kevrekidis, B. Sandstede, Counting eigenvalues via the Krein signature in infinite-dimensional Hamiltonian systems, *Physica D* 195 (2004) 263–282.
- [29] T. Kapitula, P. Kevrekidis, B. Sandstede, Addendum: counting eigenvalues via the Krein signature in infinite-dimensional Hamiltonian systems, *Physica D* 201 (2005) 199–201.
- [30] D.E. Pelinovsky, Inertia law for spectral stability of solitary waves in coupled nonlinear Schrödinger equations, *Proc. Roy. Soc. A* 461 (2005) 783–812.
- [31] M. Chugunova, D.E. Pelinovsky, Count of eigenvalues in the generalized eigenvalue problem, *J. Math. Phys.* 51 (2010) 052901.
- [32] T. Kapitula, K. Promislow, Stability indices for constrained self-adjoint operators, *Proc. Amer. Math. Soc.* 140 (2012) 865–880.
- [33] T. Kato, *Perturbation Theory for Linear Operators*, Springer, New York, 1976.
- [34] J.L. Marzuola, M.I. Weinstein, Long time dynamics near the symmetry breaking bifurcation for nonlinear Schrödinger/GrossPitaevskii equations, *Discrete Contin. Dyn. Syst. A* 28 (2010) 1505–1554.